

UNIVERSITY OF GAZIANTEP
GRADUTE SCHOOL OF
NATURAL & APPLIED SCIENCE

FRACTURE BEHAVIOR OF HIGH STRENGTH CONCRETES
CONTAINING SILICA FUME AND METAKAOLIN

M.Sc. THESIS
IN
CIVIL ENGINEERING

BY
MUDHER QAYS ABDULLAH

JUNE 2013

**Fracture Behavior of High Strength Concretes Containing Silica
Fume and Metakaolin**

M.Sc. Thesis

In Civil Engineering

University of Gaziantep

Supervisor

Assoc. Prof. Dr. Erhan GÜNEYİSİ

By

Mudher Qays ABDULLAH

June 2013

© 2013 [Mudher Qays ABDULLAH]

REPUBLIC OF TURKEY
UNIVERSITY OF GAZIANTEP
GRADUATE SCHOOL OF NATURAL & APPLIED SCIENCES
CIVIL ENGINEERING DEPARTMENT

Name of the thesis: Fracture Behavior of High Strength Concretes Containing Silica Fume and Metakaolin


Name of the student: Mudher Qays ABDULLAH

Exam date: 13.June.2013

Approval of the Graduate School of Natural and Applied Sciences


Assoc. Prof. Dr. Martin BEDİR
Director

I certify that this thesis satisfies all the requirements as thesis for the degree of Master of Science.


Prof. Dr. Mustafa GÜNAL
Head of Department

This is to certify that we have read this thesis and that in our opinion it is fully adequate, in scope and quality, as a thesis for the degree of Master of Science.


Assoc. Prof. Dr. Erhan GÜNEYİSİ
Supervisor

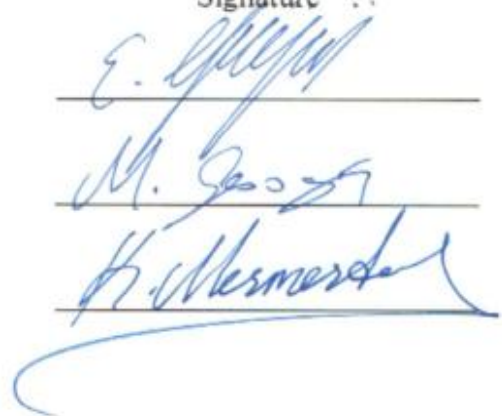
Examining Committee Members

Signature ..

Assoc. Prof. Dr. Erhan GÜNEYİSİ

Assoc.Prof. Dr. Mehmet GESOĞLU

Assist. Prof. Dr. Kasm MERMERDAŞ


The signatures of the examining committee members are written on horizontal lines. The first signature is Erhan Güneyisi, the second is Mehmet Gesoğlu, and the third is Kasm Mermerdaş.

I hereby declare that all information in this document been obtained and presented in accordance with academic rules and ethical conduct. I also declare that, as required by these rules and conduct, I have fully cited and referenced all material and results that are not original to this work.

Mudher Qays ABDULLAH

ABSTRACT

Fracture behavior of high strength concretes containing silica fume and metakaolin

ABDULLAH, Mudher Qays

M.Sc. in Civil Engineering

Supervisor: Assoc. Prof. Dr. Erhan GÜNEYİSİ

June 2013, 58 pages

The study presented in this thesis reports the findings of an experimental study conducted on fracture behavior of high strength concretes incorporating metakaolin (MK) and silica fume (SF). The concrete mixtures with water-to-binder (w/b) ratio of 0.28 and 570 kg/m³ binder content were designed for the experimental study. MK or SF modification was achieved through replacing Portland cement (PC) with mineral admixture by 5% and 15% of the total binder content. Moreover, a plain concrete mixture was produced as control for comparison. The effectiveness of MK and SF incorporation on the compressive strength, splitting and flexural strengths, modulus of elasticity, fracture energy, and characteristic length of concrete were monitored at the end of 28 days of water curing. The results have revealed that the utilization of mineral admixtures provided improvement in fracture properties such as increased fracture energy. Moreover, the results obtained for SF concretes demonstrated a similar trend to the ones incorporating MK. Increasing the replacement level from 5% to 15% resulted in relatively better performance for the concretes including mineral admixture.

Keywords: Mechanical characterization, Fracture mechanic, High strength concrete, Metakaolin, Silica fume

ÖZET

Silis dumanı ve metakaolin içeren yüksek dayanımlı betonların kırılma davranışlarının araştırılması

ABDULLAH, Mudher Qays

Yüksek lisans tezi, İnşaat Mühendisliği

Danışman: Doç. Dr. Erhan GÜNEYİSİ

Haziran 2013, 58 sayfa

Bu tezde metakaolin (MK) ve silis dumanı (SD) içeren yüksek dayanımlı betonların kırılma davranışlarının deneysel olarak incelendiği bir çalışma sunulmuştur. Deneysel çalışma için su-bağlayıcı oranı (s/b) 0.28 ve toplam bağlayıcı miktarı 570 kg/m³ alınarak beton karışımları tasarlanmıştır. MK ve SD'nin beton üzerindeki etkisini görmek amacıyla, bu mineral katkı malzemeleri %5 ve %15 oranlarında toplam bağlayıcı miktarına göre çimentoyla ağırlıkça yer değiştirilerek kullanılmışlardır. Ayrıca, karşılaştırma amaçlı olarak MK ve SD içermeyen yalın bir beton karışımı da kontrol beton olarak üretilmiştir. MK ve SD'nin etkilerini incelemek amacıyla 28 günlük kür süresi sonunda betonların basınç dayanımı, yarma ve eğilmede çekme dayanımları, elastisite modülleri, kırılma enerjileri ve karakteristik boylarındaki değişimler incelenmiştir. Sonuçlara göre mineral katkı malzemesi kullanılarak üretilen betonlarda daha yüksek kırılma enerjisi elde edilmiştir. Bunun yanısıra MK içeren betonlar SD içerenlere göre benzer davranış göstermişlerdir. Mineral katkı içeren betonlarda değişim düzeyinin %5'ten %15'e çıkarılması beton performansının daha da iyileşmesine yol açmıştır.

Anahtar kelimeler: Mekanik karakterizasyon, Yüksek dayanımlı beton, Kırılma mekaniği, Metakaolin, Silis dumanı

To My Parents , They should receive my greatest appreciation for their enormous love. They always respect what i want to do also give me their full support encouragement over the years.

ACKNOWLEDGEMENTS

First praise is to **ALLAH**, the almighty on whom ultimately we depend for sustenance and guidance. I am ever grateful to god the creator and to whom I owe my very existence.

I would like to express my highest appreciation to my supervisor Associate Prof. Dr. **ERHAN GÜNEYİSİ** for his continued encouragement and supervision.

I don't forget to thank and appreciation Assoc. Prof. Dr. **MEHMET GESOĞLU** for his encouragement and supporting.

Deep appreciation and thanks to Assist. Prof. Dr. **KASIM MERMERDAŞ** who's added me in so many ways. I would not have finished this thesis without his help, advice and guidance.

Finally, thanks and respect for my wife and my kids who helped me in completing this study.

CONTENTS

ABSTRACT	I
ÖZET	II
ACKOWLEDEGEMENTS	VIII
CONTENTS	IX
LIST OF FIGURES	XI
LIST OF TABLES	XIV
LIST OF SYMBOLS	XV
CHAPTER 1	1
1.INTRODUCTION	1
1.1 General	1
1.2. Research Significance	4
1.3. Outline of the thesis	4
CHAPTER 2	5
2. LITRATURE REVIEW AND BACKGROUND	5
2.1. Basics of fracture mechanic.....	5
2.2. Fracture properties of concrete	7
2.3. Effect of mineral admixture on mechanical properties of concrete.....	12
2.3.1. Effect of mineral admixture on compressive strength	12
2.3.2. Effect of mineral admixture on splitting tensile strength	15
2.3.3. Effect of mineral admixture on modulus of elasticity strength	17
2.3.4. Effect of mineral admixture on flexural strength	20

2.3.5. Effect of mineral admixture on fracture energy	22
2.3.6. Effect of mineral admixture on characteristic length	23
CHAPTER 3	26
3. Experimental Study	26
3.1. Materials	26
3.2. Mix proportioning and casting of concrete	29
3.3 Test methods	31
3.3.1 Compressive strength	31
3.3.2 Splitting tensile strength	31
3.3.3 Modulus of elasticity	32
3.3.4 Flexural strength	33
CHAPTER 4	38
4. Test Results and Discussions	38
4.1. Compressive Strength	38
4.2. Splitting Tensile Strength	39
4.3. Flexural Strength	40
4.4. Modulus of Elasticity	41
4.2. Fracture Parameters	42
4.2.1. Fracture energy (G_F)	42
4.2.2. Characteristic Length (l_{ch})	45
CHAPTER 5	47
5. Conclusions	47
REFERENCES	49

LIST OF FIGURES

	Page
Figure 2.1 Schematic plate of glass (Kumar and Barai, 2011)	6
Figure 2.2 Crack modes: (a) Opening mode (Mode I), (b) In-plane shear mode ,i.e. sliding (Mode II), (c) Anti-plane shear mode, i.e. tearing (Mode III) (Kumar and Barai, 2011)	7
Figure 2.3 Example of mesh sensitivity (Bazant and Cedolin, 1991)	8
Figure 2.4 Views of (a) Variation of at the crack tip in an elastic body, (b) cracked plate under tension, (c) comparison between ultimate values of applied tension, calculated according to fracture mechanics and tensile strength, (d) effect of plate width for geometrically similar plates (Cedolin, 1986)	11
Figure 2.5 Structure of crack front in ordinary cement paste and in silica fume cement paste (Bache, 1986)	12
Figure 2.6 The relationship between 28-day compressive strength and replacement level of SF (Bhanja and Sengupta, 2004)	14
Figure 2.7 Effect of SF and curing age on compressive strength of pastes (Yanjun and Cahyadi, 2003)	14
Figure 2.8 Effectiveness of metakaolin on compressive strength of concretes with different w/b ratio (Ghorpade and Rao, 2011)	15
Figure 2.9 The relation between 28-day splitting tensile strength and replacement level SF (Bhanja and Sengupta, 2004)	17

Figure 2.10	Test results on modulus of elasticity of control, MK and SF concretes at 28 days of curing age (Justice et al., 2005)	20
Figure 2.11	Variation of peak modulus of rupture versus age of concrete for a) w/cm ratio of 0.40, b) w/cm ratio of 0.50, and c) w/cm ratio of 0.60 (Justice et al., 2005)	21
Figure 2.12	Effect of maximum aggregate size on the variation of fracture energy in HPC and HSFC (Rao and Prasad, 2002)	23
Figure 2.13	The effect of compressive strength of concrete on characteristic length (Wu et al., 2001)	24
Figure 2.14	Characteristic lengths of SFRCs depending on water/cement ratio and fiber volume fraction (Şahin and Köksal, 2011)	25
Figure 3.1	Photographic views of Portland cement (PC), metakaolin (MK), and silica fume (SF)	27
Figure 3.2	Grading of aggregate	28
Figure 3.3	Compressive strength test device	32
Figure 3.4	Splitting tensile strength test configuration	
Figure 3.5	Measuring of modulus of elasticity	33
Figure 3.6	Photographic view of universal testing device and three point flexural testing fixture	34
Figure 3.7	Notched beam spaceman	35
Figure 3.8	Photographic views of notched beam specimen	36
Figure 3.9	Photographic views of LVDT	36
Figure 4.1	Variation in compressive strength of concretes containing SF and MK at 28 days	39
Figure 4.2	Variation in splitting tensile strength of concretes containing	39

	SF and MK at 28 days	
Figure 4.3	Variation in net flexural tensile strength of concretes containing SF and MK at 28 days	41
Figure 4.4	Variation in modulus of elasticity of concretes containing SF and MK at 28 days	42
Figure 4.5	Effect of MK or SF incorporation on the load-deflection behavior of the concretes	43
Figure 4.6	Variation in area under load-displacement curves of concretes containing SF and MK at 28 days	44
Figure 4.7	Variation in final displacement of beam specimens	44
Figure 4.8	Variation in fracture energies (G_F) of the concretes containing SF and MK at 28 days	45
Figure 4.9	Variation in characteristics lengths of the concretes containing SF and MK at 28 days	46

LIST OF TABLES

	Page
Table 2.1 Modulus of elasticity of concrete measured at the end of 28 days of curing (Almusallam et al., 2004)	19
Table 3.1 Properties of Portland cement, silica fume, and metakaolin	27
Table 3.2 Sieve analysis and physical properties of aggregates	29
Table 3.3 Mix proportions (kg/m ³)	30

LIST OF SYMPOLS

ASTM	American Society for Testing and Materials
CH	Calcium hydroxide
CS	Compressive strength
E	Modulus of elasticity
f_s	Splitting tensile strength
G_F	Fracture energy
HPC	High performance concrete
HSC	High strength concrete
LEFM	Linear elastic fracture mechanics
l_{ch}	Characteristic length
LVDT	Linear variable displacement transducers
MK	Metakaolin
MIP	Mercury intrusion porosimeter
OPC	Ordinary Portland cement
SP	Superplasticizer
SF	Silica fume
TPFM	Two-parameter fracture model
W/C	Water cement ratio
W/B	Water binder ratio

CHAPTER 1

1. INTRODUCTION

1.1. General

As a result of progressive development in the technology, sustainable construction has become an indispensable part of civilization. Soaring demand for more durable and long lasting structures led the formulators to investigate the practical utilization of contemporary materials of construction in civil engineering applications. Hence, high performance concrete (HPC) with superior durability and mechanical characteristics may be taken into account as a considerable components of reinforced concrete applications. It is well defined that the utilization of supplementary cementitious mineral admixtures is indispensable requirement for production of HPC (Mehta and Monteiro, 2006).

Since the middle of 1990s, the use of metakaolin (MK) as a supplementary cementitious material to provide an additional performance to concrete has attracted the interests of many researchers (Caldoarone et al., 1994; Kostuch et al., 1993; Zhang and Malhotra, 1995; Wild et al., 1996; Kakali et al., 2001; Babir et al., 2001; Barnes et al., 2003; Badogiannis et al., 2005; Poon et al., 2006; Hubertova and Hela, 2007; Güneyisi and Mermerdaş, 2007; Kim et al., 2007; Güneyisi et al., 2008; Güneyisi et al., 2010; Shekarchi et al., 2010; Güneyisi et al., 2012a; Güneyisi et al., 2012b; Mermerdaş et al., 2012; Güneyisi et al., 2013). MK is distinguished from other natural or artificial mineral admixtures in such a way that it needs a series of

processes to get pozzolanic property. Metakaolin is activated by thermal process called calcination within the temperature range 650–800 °C (Wild et al., 1996). Thermal activation process of the kaolin is basically dependent on the mineralogical structure (Sabir et al., 2001; Shvarzman et al., 2003; Badogiannis et al., 2005; Güneyisi et al., 2012b). Akin to silica fume (SF), MK has a tendency to react with portlandite (CH) formed in the hydration process, to create extra cementitious products that modify the micro-structure of concrete and accordingly enhance its overall mechanical and durability performance (Zhang and Malhotra, 1995; Barnes et al., 2003; Hubertova and Hela, 2007; Güneyisi et al., 2008).

It is well known that SF has important contribution on the improvement of interfacial transition zone between the paste and aggregate (Al-Khaja, 1994; Khatri et al., 1997; Alexander and Magee, 1999). Therefore, it has been used as a cement replacement material in the HPC production. Bhanja and Sengupta (2005) reported mechanical properties of concretes produced with the water–binder ratios ranged between 0.26 and 0.42 with different silica fume to binder ratios. They determined compressive, flexural, and splitting tensile strengths at the end of 28 days. It was reported that the strength properties were improved with silica fume incorporation. Poon et al. (2006) performed an experimental study on pore structure of high performance concretes including MK and SF. Mercury intrusion porosimeter (MIP) was utilized to monitor the pore size distribution in the concrete. The addition of MK in the cement pastes resulted in a very dense microstructure of the paste, with a lower total porosity and finer pore size distribution compared with the plain Portland cement pastes and SF blended cement pastes.

Formation of crack is one of the basic properties of concrete structures. Even under regular service loads, concrete structures can be full of cracks. Obviously, crack formation and propagation mechanism have to be taken into account for anticipating the ultimate load carrying capacity. Therefore, it can be claimed that investigating the basics of fracture mechanics for concrete can be a handful tool for a designer due to the insight it provides on how the size of a structural element affects the load capacity under service. Besides, fracture mechanics may provide solid criteria for the estimation of crack propagation. Improving the structural performance and resistance as well as diminishing cracking and spalling phenomena can be possible by increasing the concrete's toughness, ductility, tensile strength, and flexural strength under various kinds of loading (Babanajad et al., 2012).

The strength and durability behavior of MK modified concretes is known to be improved (Kostuch et al., 1993; Poon et al., 2006; Güneyisi and Mermerdaş, 2007; Güneyisi et al, 2008; Mermerdaş et al., 2012). However, the detailed information on the fracture properties of the concretes incorporating MK can be barely found in the literature. In this study, a comparative experimental study was carried out on the mechanical and especially fracture properties of concretes incorporating MK or SF as well as plain ones. In order to observe the effectiveness of MK and SF on the characteristics of the concretes, two replacement levels of mineral admixture substitution levels, namely 5% and 15%, were assigned. The tests were carried out on different types of concretes at the end of 28 days of water curing. The investigated properties are compressive strength, splitting tensile strength, flexural strength, modulus of elasticity, load displacement relations and corresponding fracture parameters such as fracture energy and characteristic length.

1.2. Research Details

In this thesis, the mechanical and fracture properties of concrete produced with mineral admixture were investigated. The compressive, splitting tensile, modulus of elasticity and flexural strengths are studied for mechanical properties of concrete. Fracture mechanic parameters such as fracture energy and characteristic length are also determined. To improve the mechanical behavior and fracture properties of mineral admixed concrete manufactured by using silica fume and metakaolin. The concrete mixtures with constant water-binder ratio of 0.28 were produced considering two replacement levels of 5% and 15% silica fume or metakaolin to investigate aforementioned properties at end of 28-day water curing period.

1.3. Outline of the thesis

Chapter 1-Introduction : Aim and objectives of the thesis are introduced.

Chapter 2-Literature review and background : A literature survey is conducted on fracture properties. The previous studies on the use of silica fume and metakaolin in concrete are provided.

Chapter 3-Experimental study : Material, mixture, casting, curing condition, and test methods are described.

Chapter 4-Test results and discussions : Indication, evaluation, and discussion of the test results are presented.

Chapter 5-Conclusion : Conclusion of the studies are given.

CHAPTER 2

2. LITRATURE REVIEW AND BACKGROUND

2.1. Basics of fracture mechanics

Fracture mechanics is a science that deals with the mechanical properties of the material and structure which gives the leverage of the state of cracks or defects develop in the body system (Kumar and Barai, 2011).

It is significant to investigate how cracks occur and propagate since they may cause structures or materials to fail. For example, a large structure, such as a bridge or a building cracks and this may lead to a catastrophic failure which might result in loss of lives. A scientist named Inglis, conducted a research on a thin plate of glass with an elliptical hole in the middle in a new and different way, in 1913. In the study, the plate was theoretically infinitely large and the hole was very small when compared to plate. Both ends of the plate was pulled at perpendicular to the ellipse (Figure 2.1). He found out that point A, at the end of the ellipse, was experiencing the highest pressure. It was also reported that as the ratio of a/b increases (the ellipse gets longer and thinner) that the stress at point A becomes greater and greater. Pulling the plate in a direction parallel to the ellipse does not cause a great stress at A. This leads to the fact that a load perpendicular, not parallel, to the crack will make it grow (Kumar and Barai, 2011).

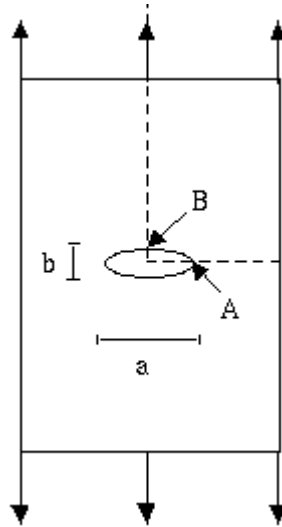


Figure 2.1 Schematic plate of glass (Kumar and Barai, 2011)

The behavior of materials alters, once a crack starts to grow. The variations occur in the resistance of materials; the energy necessary to grow the crack might also fluctuate up or down. In order for the crack to have progressive increase each time, the energy change must be equal to the change of resistance. Unless more force is applied the crack does not grow any more in case the change in energy is lower than the change in resistance. However, an unstable crack growth is observed when the change in energy is greater than the change in resistance. Hence, the crack keeps growing until the structure fails (Kumar and Barai, 2011).

Linear elastic fracture mechanics (LEFM) approach has been developed since the end of the last century. LEFM is utilized especially in structural steel design for simulation of the quasibrittle materials. Such materials like fibrous concrete, rock and engineered cementitious materials need some factors and a new approach to understand the mechanical fracture (Kumar and Barai, 2011).

On the basis of the available analytical procedures, Irwin (1957) developed the linear elastic crack stress fields and demonstrated that the stress field near a sharp crack tip is depended on a different boundary condition of body, kind of cracking mode, loading, and geometry. Cracking modes are sorted in the modes given below in Figure 2.2.

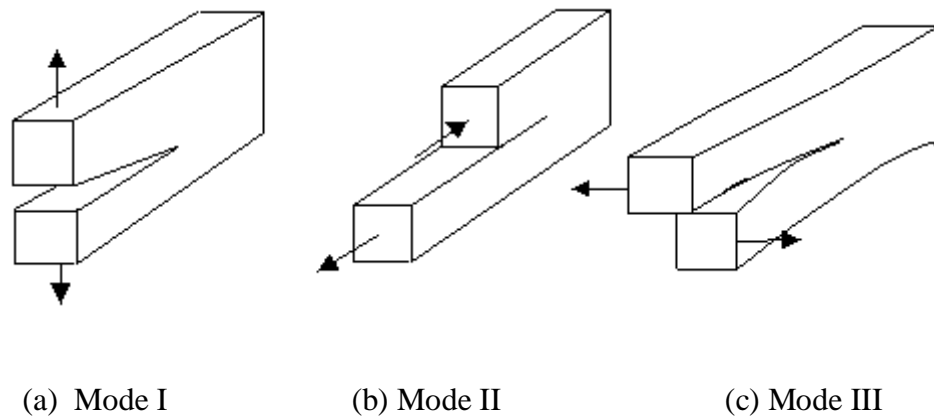


Figure 2.2 Crack modes: (a) Opening mode (Mode I), (b) In-plane shear mode , i.e. sliding (Mode II), (c) Anti-plane shear mode, i.e. tearing (Mode III) (Kumar and Barai, 2011)

2.2. Fracture properties of concrete

Applying fracture mechanics to concrete design can provide much insight on how the size of a structural element may affect the ultimate load capacity. It can also be a useful tool in predicting crack propagation. Consider a case where you are responsible for determining if a given crack in a large structure such as a concrete dam will propagate catastrophically under certain loading conditions. You can adopt a strength criterion that predicts that a crack will propagate when the stresses reach the ultimate tensile strength of the material. For sharp cracks, however, the theory of

linear elasticity predicts that the stresses at the tip of the crack go to infinity, thereby assuming that the crack will propagate no matter how small the applied stress, an unlikely scenario. Fracture mechanics, on the other hand, provides an energy criterion that does not have such drawbacks and allows for more precise predictions of the stability of the crack. The application of this energy criterion can be particularly useful when using traditional finite element methods to study cracks where mesh sensitivity becomes a problem. Figure 2.3 shows an example where the result is greatly affected by the size of the mesh when a strength criterion is used, however, little mesh sensitivity is observed when an energy criterion based on fracture mechanics is employed (Mehta and Monteiro, 2006).

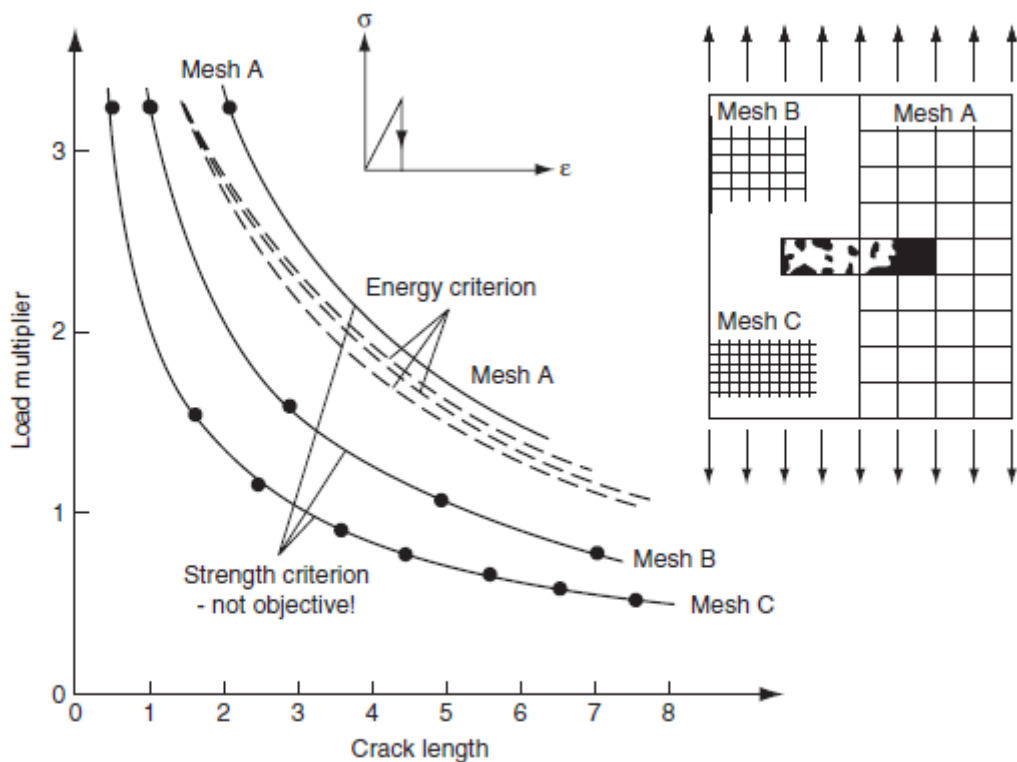


Figure 2.3 Example of mesh sensitivity (Bazant and Cedolin, 1991)

Considering the advantages of using fracture mechanics for concrete, it is surprising that this is a relatively new area of research. The development of fracture mechanics for concrete was slow as compared to other structural materials. Throughout the last two decades, intensive research has been performed and applications of fracture mechanics in the design of beams, anchorage, and large dams are becoming more common. That said, when compared to previous continuum theories covered in this chapter (elasticity, viscoelasticity, and thermal problems), fracture mechanics is not yet as mature a theory and this will be reflected in its presentation. A fair, but simplified, exposition of some of the existing fracture mechanics models for concrete are presented later at an introductory level (Mehta and Monteiro, 2006).

Concrete contains many flaws, pores, and other non-homogeneities. It fails under compression and/or tension by a process of continuous micro cracking with extreme complexity, which includes slow crack propagation and local damage of materials before the global failure (Bazant, 2002).

Pores in hardened cement paste and restrained shrinkage induced cracking have important impact on the mechanical features of concrete. These cracks and defects are significant factors resulting in the failure of the material body, especially when repeated load on specimen, The growth of these cracks in a certain place called fracture process zone (Kumar and Barai, 2011).

Many research and experiments have shown that the most familiar form of LEFM philosophy cannot be applied to concrete members with normal size. This is because of the fact that LEFM was discovered and reasoned as the availability of large and variable size of fracture process zone (Kumar and Barai, 2011). By beneficitation of nonlinear fracture mechanics principles, Hillerborg et al. (1976) offered an approach

through development of fictitious crack model based on cohesive crack model (Dugdale, 1960; Barenblatt, 1962) for the crack propagation study of unreinforced concrete beam.

The first experimental research on fracture mechanics of concrete was performed by Kaplan in 1961 (Mehta and Monteiro, 2006). Subsequent research studied the effects of various parameters on K_C and G_C . Experimental studies indicated that the fracture toughness increases with increasing (a) aggregate volume (b) maximum-size aggregate, and (c) roughness of the aggregate. As expected, the toughness decreases with increasing water-cement ratio and increasing air content. One of the problems encountered in the early stages of the research was that, instead of being a material property, the value of the fracture toughness K_C , was strongly influenced by the size of the specimen tested. It soon became apparent that fracture mechanics measurements should not be made on small concrete specimens. Cedolin (1986) analyzed what happens to the ultimate stress when the dimensions of a cracked plate was changes. His analytical study is summarized in Figure 2.4.

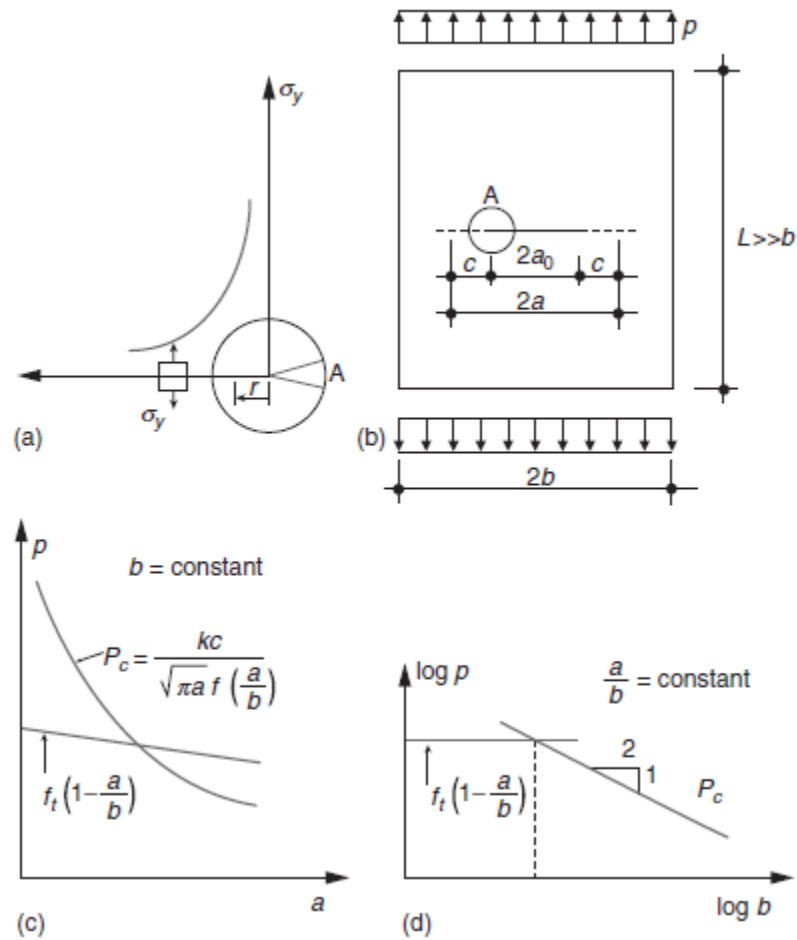


Figure 2.4 View of (a) Variation of σ_y at the crack tip in an elastic body, (b) cracked plate under tension, (c) comparison between ultimate values of applied tension, calculated according to fracture mechanics and tensile strength, and (d) effect of plate width for geometrically similar plates (Cedolin, 1986)

It is convenient to define a brittleness number, to characterize the nature of the collapse; the lower the brittleness number the more brittle the behavior of the specimen. Fracture occurs in specimens with a small brittleness number, that is, for materials with a comparatively low fracture toughness, a high tensile strength, and in large specimens. The brittleness number characterizes the nature of the collapse for one-dimensional problems; for beams or slabs in flexure, additional information on

the slenderness is necessary. This number helps to explain the experimental results where concretes made with high-strength silica fume cement paste usually have more fine microcracks than normal strength concrete (Figure 2.5). In the high-strength matrix, the tensile strength can be two to five times greater than the normal-strength matrix; however, the increase in fracture energy or elastic modulus is not as much. Consequently, a high-strength matrix has much lower brittleness number and is more susceptible to the development of cracks. A complete description of scaling flaws for brittle materials is given by Bazant. Structure of the crack front in plain cement paste and silica fume cement paste was graphically demonstrated by Bache (1986) as seen in Figure 2.5.

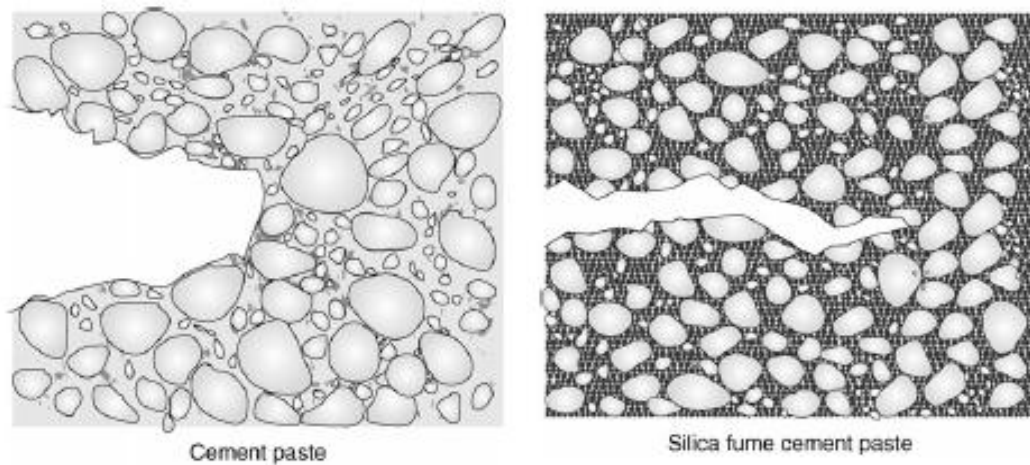


Figure 2.5 Structure of crack front in ordinary cement paste and in silica fume cement paste (Bache, 1986)

2.3. Effect of mineral admixture on mechanical properties of concrete

2.3.1. Effect of mineral admixture on compressive strength

Bhanja and Sengupta (2005) carried out an extensive experimental study on the concretes with various water–binder ratios between 0.26 and 0.42. Moreover, they utilized SF as mineral admixture with SF–binder ratios from 0.0 to 0.3. For all of the mixtures, they determined the compressive strengths at the end of 28 days of curing. They concluded that compressive strength of concrete is increased with silica fume inclusion. The results also demonstrated that although the optimum replacement level is not constant, it is dependent of the water to cementitious material (w/cm) ratio of the concrete. The highest compressive strength was measured as 95.7 MPa at 15% replacement level for the concrete with w/cm ratio of 0.26, while the lowest compressive strength of 48.3 MPa was measured for the control concrete at w/cm ratio of 0.42 as shown in Figure 2.6.

The compressive strength results reported in the study of Yanjun and Cahyadi (2003) are depicted in Figure 2.7, indicating SF replacement levels ranging between 0-20% and by weight of cement and at w/b ratio of 0.4. As it was expected the compressive strength of five different types of mixes increased with increase in curing age. However, the influence of SF on compressive strength at early ages appeared to be insignificant. At later ages, it was obvious that SF incorporation contributed well on 56 and 90 days compressive strength of concrete.

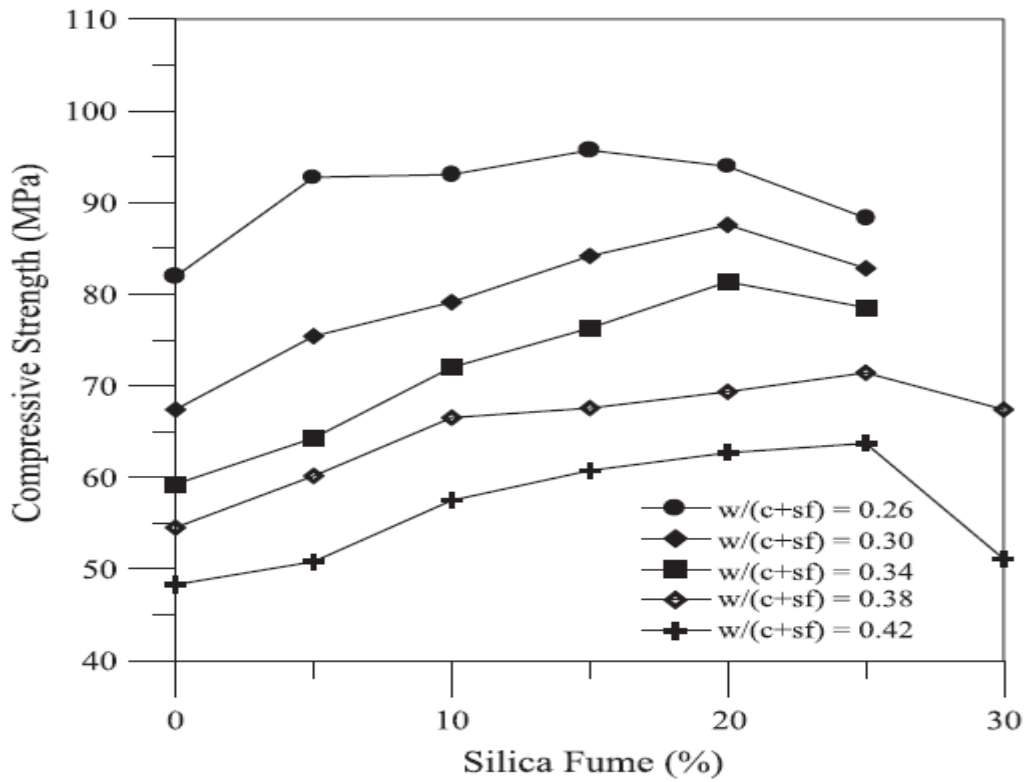


Figure 2.6 The relationship between 28-day compressive strength and replacement level of SF (Bhanja and Sengupta, 2004)

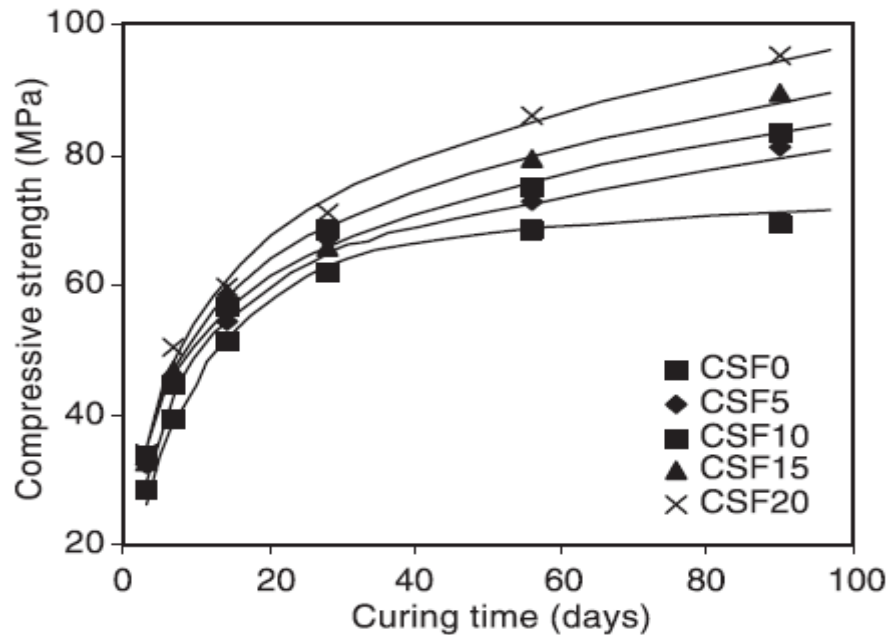


Figure 2.7 Effect of SF and curing age on compressive strength of pastes (Yanjun and Cahyadi, 2003)

In the study of Ghorpade and Rao (2011), high performance concrete with various w/b ratio and MK replacement level up to 30% were used for compressive strength testing. They determined that high strength concrete with 95.4 MPa can be achieved by adjusting w/b ratio and proper replacement level of MK (Figure 2.8).

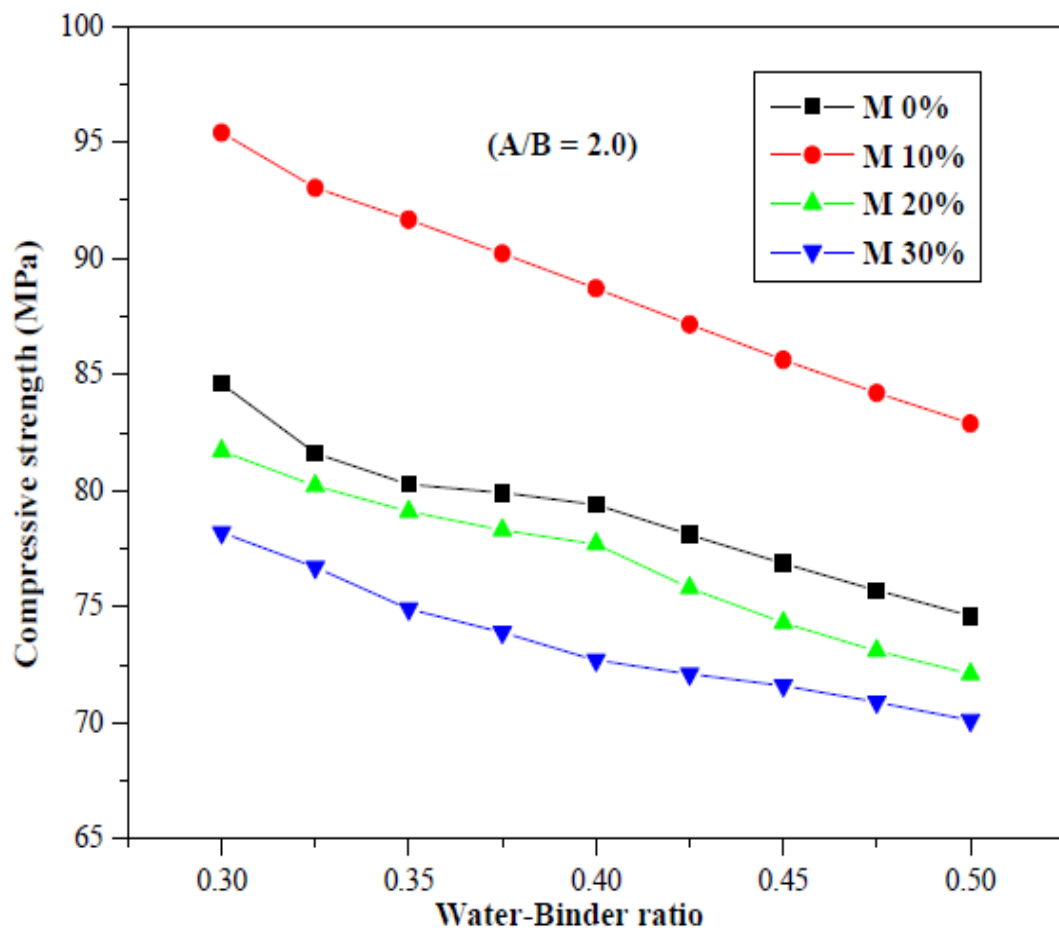


Figure 2.8 Effectiveness of metakaolin on compressive strength of concretes with different w/b ratios (Ghorpade and Rao, 2011)

2.3.2. Effect of mineral admixture on splitting tensile strength

The tensile strength of concrete can be considered as one of the basic and significant characteristics of the concrete. Besides, this parameter is used in some aspects of reinforced concrete design. Because of concrete's low tensile strength and its brittleness, concrete structures are generally designed in such a way that tensile forces act indirectly to the structural member. Nevertheless, the concrete is not usually expected to resist the direct tension because of its low tensile strength capacity it is required to decide on the critical load at which the structural concrete member may undergo cracking. The corresponding crack formation is a type of tension failure. Different from the bending test, the other test methods used for determination of the tensile strength of concrete can be categorized in two sections, namely, direct testing methods, indirect methods. The famous method of indirect testing is splitting tensile strength test. This method of testing has been largely utilized for determination of tensile strength of concrete. It is frequently used by investigators and formulators to characterize and design reinforced concrete structural members (IS 5816-1999).

An elaborate experimental study reported on splitting tensile strength of concrete was conducted by Bhanja and Sengupta (2004). The observation of the test results exhibits that very high rates of silica fume replacement does not importantly affect splitting tensile strength of concrete. Moreover, SF replacement levels higher than 20% caused decrease in the splitting tensile strength. The optimum replacement levels seemed to vary between 5-15%.

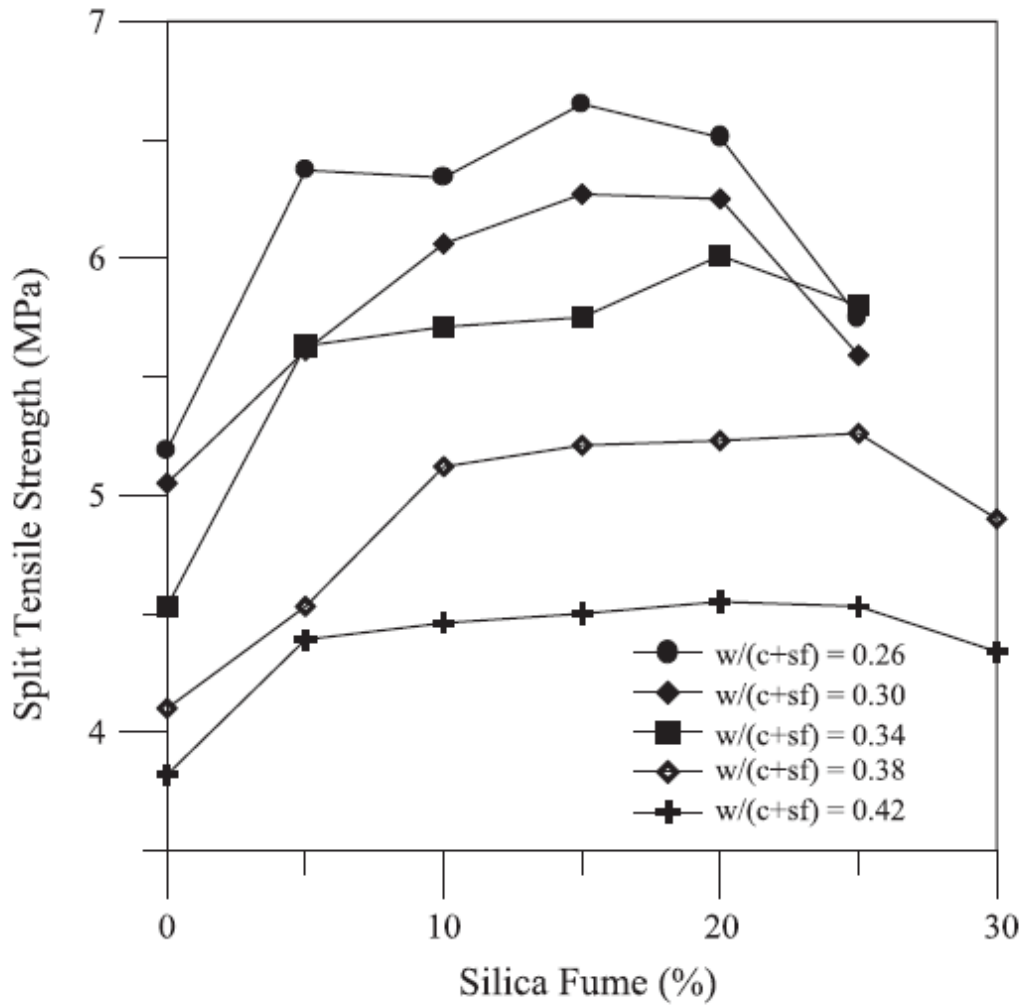


Figure 2.9 The relation between 28-day splitting tensile strength and replacement level SF (Bhanja and Sengupta, 2004)

2.3.3. Effect of mineral admixture on modulus of elasticity strength

Modulus of elasticity of concrete plays a key role for predicting the deformation behaviour of structural members and buildings. It is utilized for the design section size and shape of the members subjected to flexure. For normal strength concrete, modulus of elasticity is proportional to square root of compressive strength depending mainly on the features of the concrete (Noguchi and Nemati, 1990).

ASTM C 469 defines a standard test method for measuring the modulus of elasticity of 150 by 300 mm concrete cylinders loaded longitudinally in compression at a constant pace rate ranging between 0.24 ± 0.03 MPa/s. Normally, the deformations are measured by an LVDT. The elastic modulus values used in concrete design computations are usually estimated from empirical expressions that assume direct dependence of the elastic modulus on the strength and density of concrete. As a first approximation this makes sense because the stress-strain behavior of the three components of concrete, namely the aggregate, the cement paste matrix, and the interfacial transition zone, would indeed be determined by their individual strengths, which in turn are related to the ultimate strength of the concrete. Furthermore, it may be noted that the elastic modulus of the aggregate (which controls the aggregate's ability to restrain volume changes in the matrix) is directly related to its porosity, and the measurement of the unit weight of concrete happens to be the easiest way of obtaining an estimate of the aggregate porosity (Mehta and Monteiro, 2006).

Almusallam et al. (2004) reported that modulus of elasticity of concrete specimens change considerably with the change of aggregate type and incorporation of silica fume. Their experimental results are presented in Table 2.1. Based on the result reported in Table 2.1, it was determined that incorporation of SF contributed up to 45% increase in modulus of elasticity mainly depending on aggregate type. They measured the lowest modulus of elasticity as 21.60 GPa for concrete without SF and incorporating calcereous limestone. However, the highest modulus of elasticity (40.40 GPa) obtained for the concrete with 15% SF and produced with steel slag.

Table 2.1 Modulus of elasticity of concrete measured at the end of 28 days of curing
(Almusallam et al., 2004)

Aggregate	Modulus of elasticity, (GPa)		
	0% Silica fume	10% Silica fume	15% Silica fume
Calcareous limestone	21.60	26.00	29.30
Dolomitic limestone	24.50	25.90	32.80
Quartzitic limestone	28.80	36.20	38.00
Steel slag	29.60	32.90	40.40

In the study of Justice et al. (2005), the effectiveness of two types of metakaolin and silica fume on the modulus of elasticity of concretes with different w/cm ratios were reported. For all w/cm ratios, as shown in Figure 2.10, SF incorporated concretes revealed higher modulus of elasticity than control and MK incorporated concretes. It was also reported that the influence of MK and SF addition was mostly pronounced at w/cm ratio of 0.4. The highest modulus of elasticity values of 34 and 29 GPa were observed for MK and control concretes.

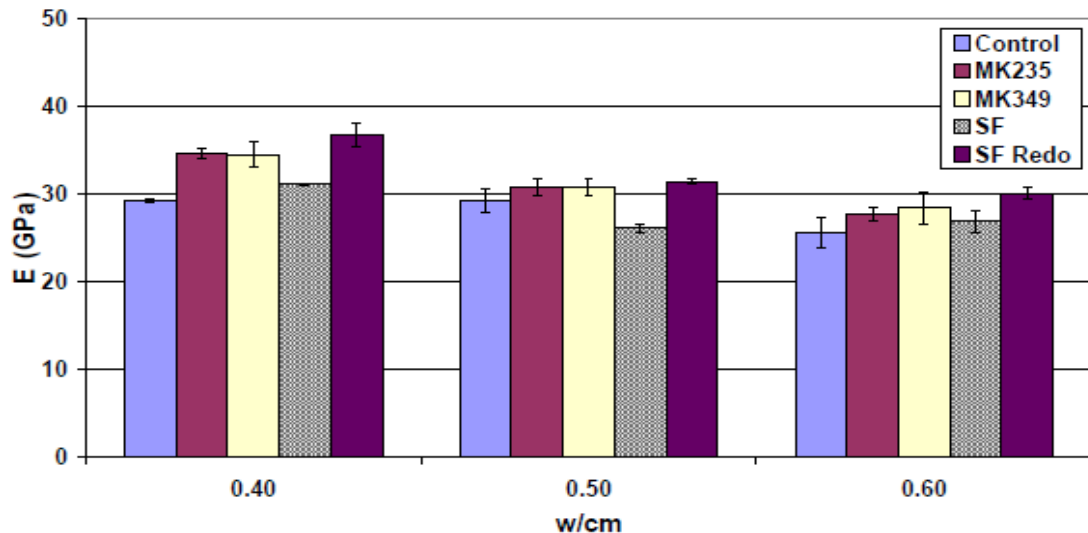
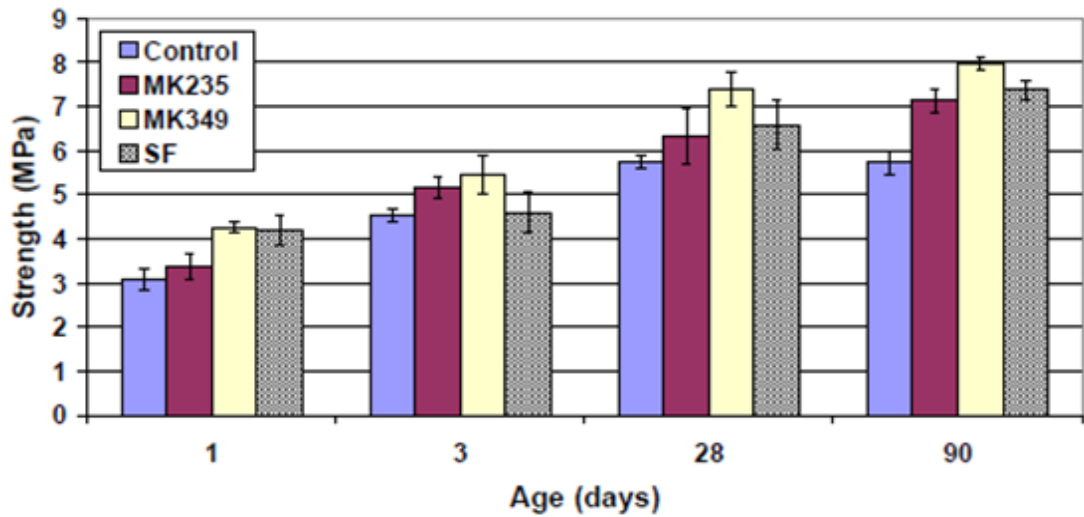


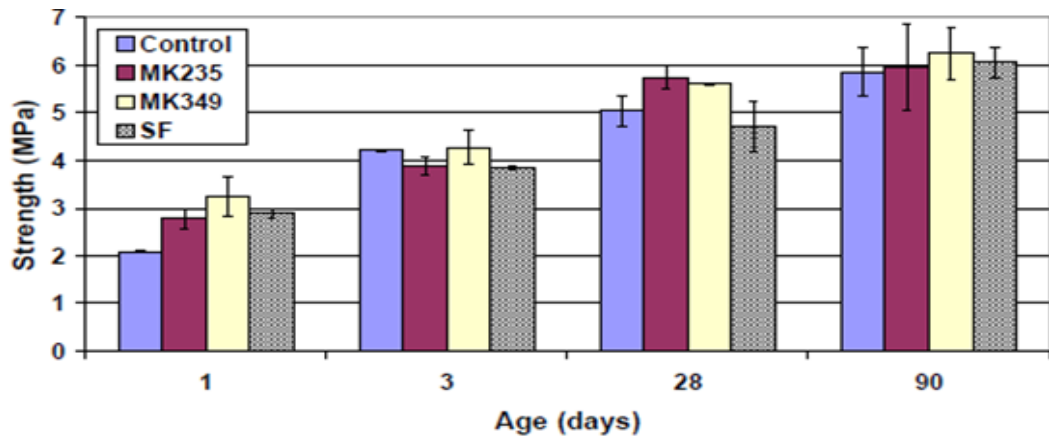
Figure 2.10 Test results on modulus of elasticity of control, MK, and SF concretes at 28 days of curing (Justice et al., 2005)

2.3.4. Effect of mineral admixture on flexural strength

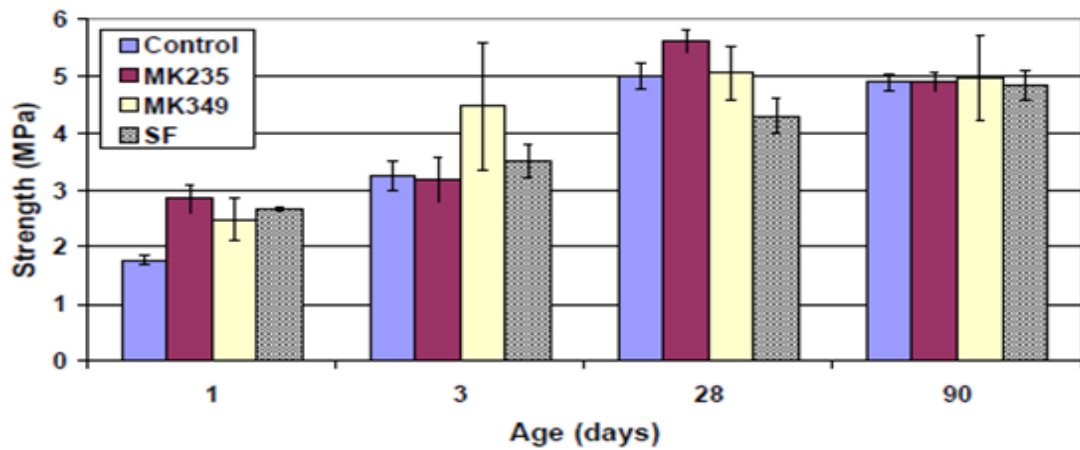
It has been known that incorporation of metakaolin generally increases the mechanical properties of concretes. In the study of Justice et al. (2005), different types of MK and SF incorporated concrete prisms were subjected to the flexural strength test. It was concluded that there was an increase of 1-2 MPa as a result of using metakaolins for the prisms subject to bending. Although they did not observe a clear tendency indicating that one of the MK used was better than the other type, they reported improvement in flexural strength capacity due to MK incorporation. Moreover, prisms produced with silica fume as a partial replacement of cement demonstrated somewhat higher flexural higher than the control at w/cm ratio of 0.40. However, concrete mixes having higher w/cm ratio were not different from control at all. It was also reported that at w/cm ratio of 0.40, MK349 and silica fume prisms had modulus of rupture values higher than 4 MPa at 24 hours after casting. Whereas, it took 3 days for control and MK235 concrete prisms to reach this value (Justice et al., 2005).



a)



b)



c)

Figure 2.11 Variation of peak modulus of rupture versus age of concrete for a) w/cm ratio of 0.40, b) w/cm ratio of 0.50, and c) w/cm ratio of 0.60 (Justice et al., 2005)

2.3.5. Effect of mineral admixture on fracture energy

It is known that a three-point flexural test applied to a notched beam yields a stable load-deflection curve. The amount of energy depleted due to the crack propagation through the notched beam specimen can be determined by calculating the area under this curve. By knowing the effective cross-sectional area the fracture energy (G_F) can be calculated (Peterson, 1980).

Change in the fracture energy due to variation of the maximum aggregate size is shown in Figure 2.12 (Rao and Prasad, 2002). The figure indicates the variation of fracture energy of concretes with and without SF. It was reported that there is an evident increase in the fracture energy as the maximum aggregate size increases. They also stated that addition of SF by 10% has considerably enhanced the strength of concrete. It was found that the fracture energy (G_F) of concrete was measured as 76.6 N/m for the concrete having maximum size of coarse aggregate equal to 4.75 mm. However, the fracture energy raised up to 142 N/m for the concrete with maximum aggregate size of 20 mm in plain concrete. Incorporation of SF resulted in increase of G_F from 122 to 165 N/m (Rao and Prasad, 2002).

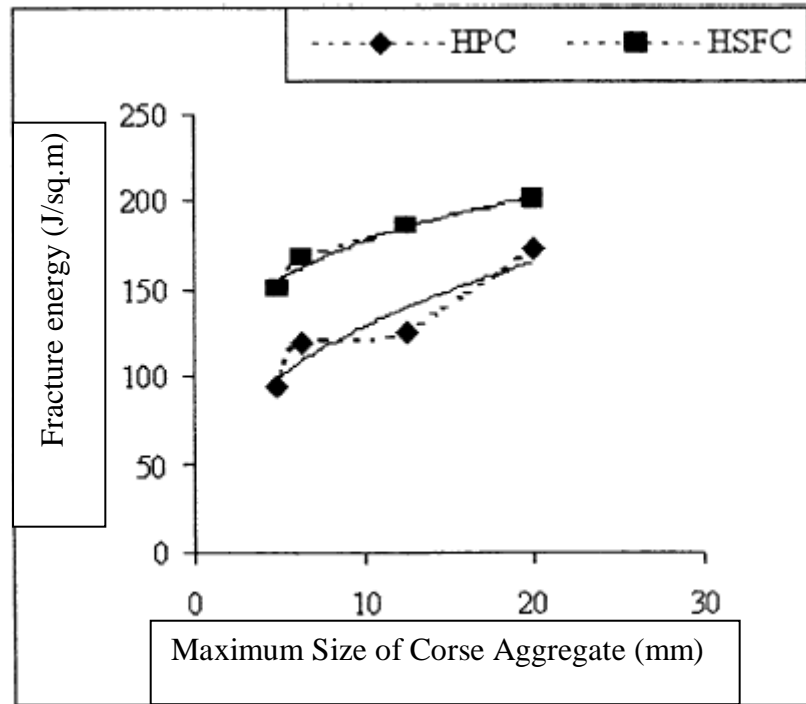


Figure 2.12 Effect of maximum aggregate size on the variation of fracture energy in HPC and HSFC (Rao and Prasad, 2002)

2.3.6. Effect of mineral admixture on characteristic length

The brittleness of concrete can be assessed by a factor named characteristic length, l_{ch} . Characteristic length can be calculated by the following relation.

$$l_{ch} = \frac{EG_F}{f_s^2} \quad (2.1)$$

Where E is the modulus of elasticity, f_s is the splitting tensile strength, and G_F is the fracture energy.

It has been reported that the higher the brittleness number (lower l_{ch}) of a given structure, the lower the ductility. Rao and Prasad (2002) conducted an experimental study on the fracture properties of high-strength concrete (HSC). Different coarse aggregate sizes were used to compare the fracture properties of HSC. For the plain

concrete without SF, the characteristic length was observed to increase as the maximum size of coarse aggregate increased, which indicates increase in the ductility.

A similar study was also reported by Wu et al. (2001) on the effects of different types of aggregate on the fracture properties. They demonstrated that the effects of the strength of concrete and the types of the aggregates on the characteristic length are troubled, the results show that the characteristic length reduces, that is, the brittleness of concrete increases, with increasing strength, as illustrated in Figure 2.13.

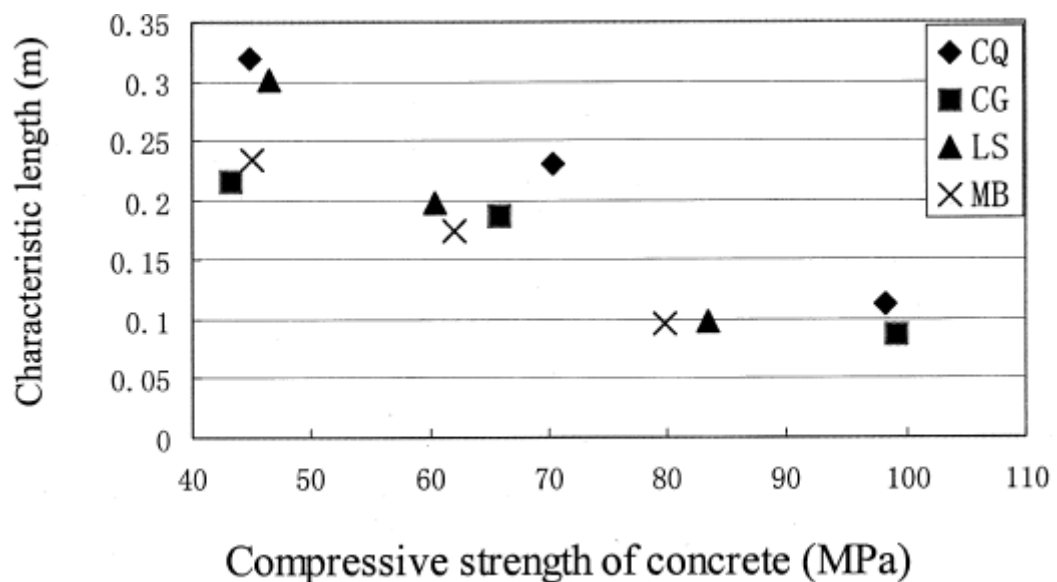
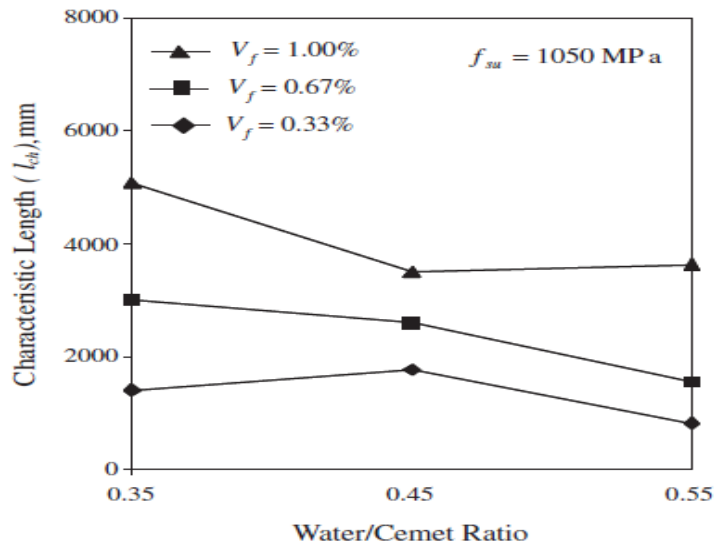


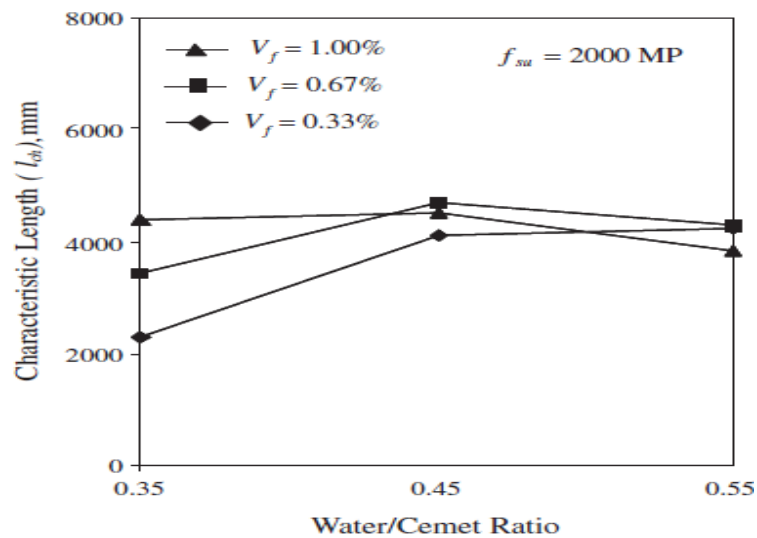
Figure 2.13 The effect of compressive strength of concrete on characteristic length
(Wu et al., 2001)

The influences of both matrix strengths and steel fiber on fracture energy of high strength concrete was experimentally evaluated in the study of Şahin and Köksal (2011). They reported that the characteristic length increases by decreasing

water/cement ratio or increasing matrix strength for the fiber tensile strength of 1050 MPa as depicted in Figure 2.14. Maximum characteristic length values are obtained at the water/cement ratio of 0.45 and for fibre having 2000 MPa tensile strength. The changes in characteristic lengths of concretes depends on the fibre volume fraction and water/cement ratio (Şahin and Köksal, 2011).



(a) $f_{su} = 1050 \text{ MPa}$



(a) $f_{su} = 2000 \text{ MPa}$

(b) Figure 2.14 Characteristic lengths of SFRCs depending on water/cement ratio and fiber volume fraction (Şahin and Köksal, 2011)

CHAPTER 3

3. EXPERIMENTAL STUDY

3.1. Materials

CEM I 42.5 R type Portland cement having specific gravity of 3.14 and Blaine fineness of 327 m²/kg was utilized for preparing the concrete test specimens used in determination of mechanical properties. The chemical composition of the cement is shown in the Table 3.1. Metakaolin (MK) used in this study is a white powder with a Dr Lange whiteness value of 87. It has a specific gravity of about 2.60, and specific surface area (Nitrogen BET Surface Area) of 18000 m²/kg. Physical and chemical properties of MK used in this study are given in Table 3.1. MK used in this study is from Czech Republic. Silica fume (SF) obtained from Norway was used as a mineral admixture in concrete production for comparing the effectiveness of MK. SF has a specific surface area of 21080 m²/kg and specific gravity of 2.2. Chemical analysis and some physical properties of SF are also given in Table 3.1. Figure 3.1 indicates the photographic views of cement and mineral admixture used.

Table 3.1 Properties of Portland cement, silica fume, and metakaolin

Chemical analysis (%)	Portland cement	Silica fume	Metakaolin
CaO	62.58	0.45	0.5
SiO ₂	20.25	90.36	53
Al ₂ O ₃	5.31	0.71	43
Fe ₂ O ₃	4.04	1.31	1.2
MgO	2.82	-	0.4
SO ₃	2.73	0.41	-
K ₂ O	0.92	1.52	-
Na ₂ O	0.22	0.45	-
Loss on ignition	1.02	3.11	0.4
Specific gravity	3.14	2.2	2.60
Fineness (m ² /kg)	327*	21080**	18000**

* Blaine specific surface area

** BET specific surface area



Metakaolin

Cement

Silica fume

Figure 3.1 Photographic views of Portland cement (pc), metakaolin (MK), and silica fume (SF)

Fine aggregate was mix of river sand and crushed sand whereas the coarse aggregate was river gravel with a maximum particle size of 16 mm. Aggregates were obtained from local sources. Properties of the aggregates are presented in Table 3.2. Grading of the aggregate mixture was kept constant for all concretes figure 3.2 shows the grading of aggregates. A polycarboxylic-ether type superplasticizer (SP) with a specific gravity of 1.07 and pH of 5.7 was used in all mixtures.

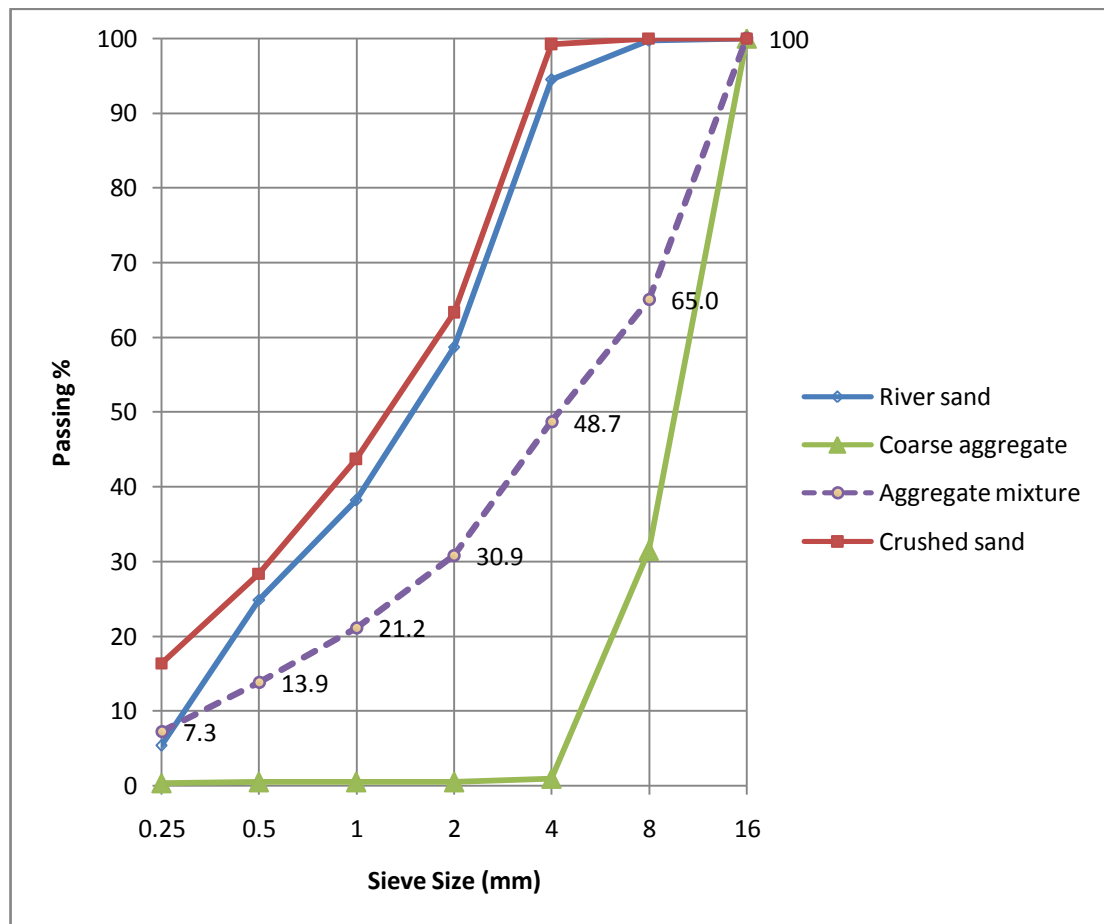


Figure 3.2 Grading of the aggregates

Table 3.2 Sieve analysis and physical properties of aggregates

Sieve size (mm)	Passing (%)		
	Fine aggregate		Coarse aggregate
	River sand	Crushed sand	
16.0	100	100	100
8.0	99.7	100	31.5
4.0	94.5	99.2	1.0
2.0	58.7	63.3	0.5
1.0	38.2	43.7	0.5
0.5	24.9	28.4	0.5
0.25	5.4	16.4	0.4
Fineness modulus	2.87	2.57	5.66
Specific gravity	2.66	2.42	2.72

3.2. Mix proportioning and casting of concrete

Concretes were designed with water-to-binder ratio of 0.28 and total binder content of 570 kg/m³. In order to develop metakaolin and silica fume modified high strength concrete mixtures, Portland cement was partially replaced with 5% and 15% mineral admixture (by weight). Considering one control mixture, thus, totally five different mixtures were prepared in this study. Details of the mixtures are given in Table 3.3. The concretes were designated by the type and the replacement level of the mineral admixture. For example, 5SF stands for the concrete group including 5% SF. The mixtures given in Table 3.3 were designed to have slump values of 100 ± 20 mm for the ease of handling, placing, and consolidation. The superplasticizer was added at the time of mixing to achieve the specified slump.

Table 3.3 Mix proportions (kg/m³).

Mix proportions	Mix ID				
	Control	5MK	15MK	5SF	15SF
Cement	570.0	541.5	484.5	541.5	484.5
Water	159.6	159.6	159.6	159.6	159.6
MK	0	28.5	85.5	0	0
SF	0	0	0	28.5	85.5
Coarse aggregate	863.1	857.8	849.2	855.3	842.1
River sand	675.3	669.7	660.3	671.8	666.7
Crushed sand	155.5	154.2	152.0	154.7	153.5
Superplasticiser	5.13	6.84	8.55	7.125	9.12

All concretes were mixed in accordance with ASTM C192 (ASTM C192/C192 M-07, 2007) standard in a power-driven revolving pan mixer and the tests were performed after 28 days of water curing periods. For each mixture, 150x150x150-mm cubes, Φ 150x300-mm cylinders, and 100x100x500 prisms were used for determination of compressive strength, splitting tensile strength and flexural strength, and fracture energy, respectively. Transverse notches having 5 mm width and 40 mm height were opened in the middle of the beam specimens one day before the testing. Three specimens were utilized for each testing.

3.3 Test methods

3.3.1 Compressive strength

The compressive strength test conforming to ASTM C39 (ASTM C39/C39M-12,2012) was carried out on cube specimens (150x150x150 mm) by a 3000 KN capacity testing machine. Figure 3.3 illustrates the compression test on concrete cube.



Figure 3.3 Compressive strength test device

3.3.2 Splitting tensile strength

Splitting tensile strength was carried out on the specimens having $\Phi 150 \times 300$ mm size according to the specification per ASTM C496 (ASTM C496,2011). Splitting tensile strength of a cylinder specimen is calculated using the following expression:

$$f_s = \frac{2P}{\pi DL} \quad (3.1)$$

where P , L , and D are the ultimate load, length and diameter of the cylinder specimen, respectively. The schematic drawing of the test specimen and configuration is given in Figure 3.4.

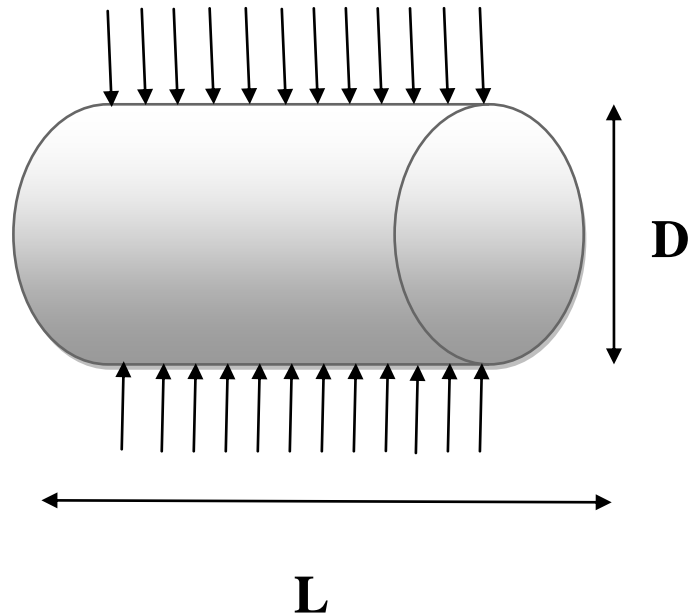


Figure 3.4 Splitting tensile strength test configuration

3.3.3 Modulus of elasticity

Cylinders with a dimension of $\Phi 150 \times 300$ mm were tested for determining the static modulus of elasticity as per ASTM C469 (ASTM 469/C469M-10,2010). Each of the specimens was fitted with a compress meter containing a dial gage capable of measuring deformation to 0.002 mm and then loaded three times to 40% of the ultimate load. The ultimate load was determined based on the compressive strength test results for each mix. The first set of readings of each cylinder was discarded and the modulus was reported as the average of the second two sets of readings. For each parameter, three specimens were used. Figure 3.5 reveals the measurement of modulus of elasticity of concrete.



Figure 3.5 Measuring of modulus of elasticity

3.3.4 Flexural strength

Three point flexural test was applied by 250 kN capacity universal testing device to obtain flexural strength and fracture parameters of the concretes (Figure 3.6). For this purpose, notched beam specimens were used (Figure 3.7). The beam length, width, and depth were 500, 100, and 100 mm, respectively. The notch opening was achieved through reducing the cross section to 60x100 mm by sawing in order to accommodate large aggregates. The flexural strength of a notched beam tested under three-point flexural test can be assessed using the following equation on the assumption that there is no notch sensitivity:

$$f_{flex} = \frac{3P_{max} S}{2B(D-a)^2} \quad (3.2)$$

Where P_{max} is the ultimate load (N), and S , B , D , and a are span length (400 mm),

width of the beam (100 mm), depth of the beam (100 mm), and notch depth (40 mm), respectively.



Figure 3.6 Photographic view of universal testing device and three point flexural testing fixture

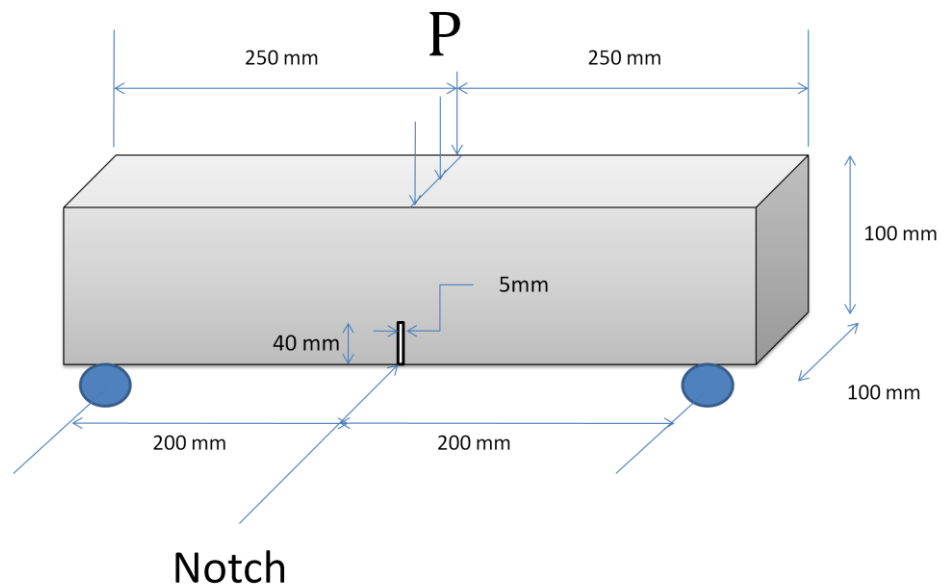


Figure 3.7 Notched beam specimen

The details of the specimen as well as placing linear variable displacement transducers (LVDTs) were shown in Figure 3.8 The test for the determination of the fracture energy (G_F) was realized based on the recommendation of RILEM 50-FMC Technical Committee (RILEM 50-FMC,1985). Deformation controlled loading was applied during the testing of the beam specimens. The constant loading rate of 0.02 mm/min up to a deflection of 1.5 mm was adopted. As seen in the photographic view of the test set up in figure 3.9, the deflection was measured by means of LVDT. The fracture energy G_F of the concrete can be calculated by the following equation:

$$G_F = \frac{W_0 + mg\left(\frac{S}{L}\right)\delta_{\max}}{A_{lig}} \quad (3.3)$$

Where W_0 is the area under the load-deflection curve (Nm), m is the mass of the specimen (kg), g is the gravitational acceleration (m/s^2), L is the total length of specimen, δ_{\max} is the maximum displacement (m), and A_{lig} is the area of the initial ligament [$B(D-a)$] (m^2); B and D are the width and depth of the beam, respectively; a is the depth of the notch.



Figure 3.8 Photographic views of notched beam specimen



Figure 3.9 Photographic views of LVDT

The fracture energy G_F alone does not provide adequate information to characterize the ductility or brittleness of concrete and its dependence on the size of the structure. Instead, the brittleness number proposed by Hillerborg (Hillerborg et al.,1976) captures both the influence of the material and that of the size of the structure by means of the ratio (Eqn 3.4):

$$\beta = \frac{l}{l_{ch}} \quad (3.4)$$

Where l is any structural dimension and l_{ch} is a material parameter known as the characteristic length, defined by the following ratio (Eqn 3.5):

$$l_{ch} = \frac{EG_F}{f_s^2} \quad (3.5)$$

Where E is the modulus of elasticity and f_s is the splitting tensile strength (In this study, splitting tensile strength was used instead of direct tensile strength).

CHAPTER 4

4. TEST RESULTS AND DISCUSSIONS

4.1. Compressive Strength

The compressive strength of the concretes measured at 28 days were presented in Figure 4.1. The compressive strength values ranged from 68.6 to 86.8 MPa, depending mainly on inclusion and replacement level of the mineral admixture. The control group had the lowest compressive strength of all, while the highest was measured for 15SF concrete. The relative compressive strengths to control were 122.3%, 126.5%, 115.9%, and 122.0% for the concretes 5SF, 15SF, 5MK, and 15MK, respectively. MK incorporated concretes revealed similar trend as SF concretes did. However, the percentage of increase was slightly different. For example, utilizing mineral admixture by 15% provided 3.5% and 5.2% more compressive strength than 5% level of replacement for SF and MK incorporation, respectively. It was reported that, the essential factors that affect the contribution of metakaolin are i) the filling effect, ii) the dilution effect, and iii) the pozzolanic reaction of metakaolin with CH (Wild et al., 1996). Although having comparable results to SF incorporated ones, MK concretes seemed to have lower compressive strength development at the end of 28 days. This may be attributed to the better pore refinement of SF due to higher specific surface area (see Table 3.1).

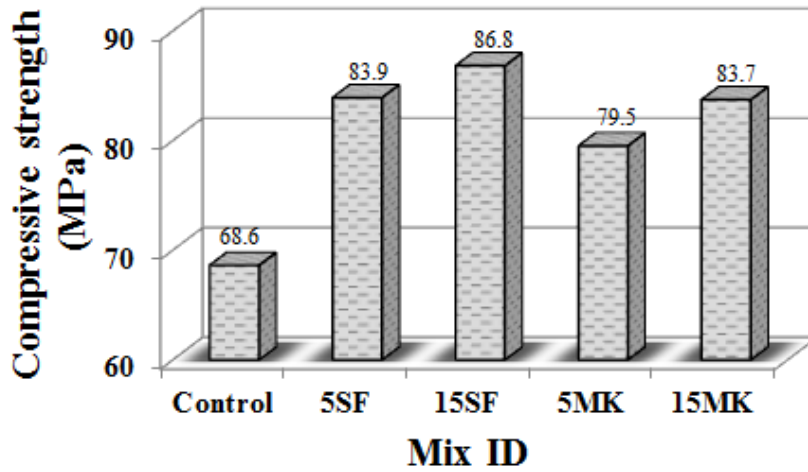


Figure 4.1 Variation in compressive strength of concretes containing SF and MK at 28 days

4.2. Splitting Tensile Strength

The indirect tensile strength of the concrete monitored by splitting test at 28 days and is graphically shown in Figure 4.2. Similar to compressive strength results, the incorporation of MK or SF provided enhancement in splitting tensile strength results.

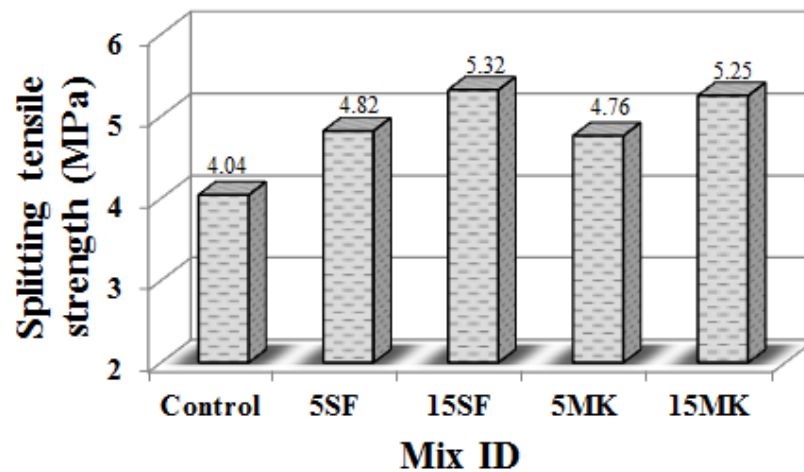


Figure 4.2 Variation in splitting tensile strength of concretes containing SF and MK at 28 days

However, the concretes having same replacement level had very close splitting tensile strength values to each other. For example, splitting tensile strength values of 5.32 MPa and 5.25 MPa was measured for 15SF and 15MK, respectively. Neville (1996) points out that there was a direct proportionality between splitting tensile and compressive strengths of concrete at different rates. In other words, while the compressive strength increased, the tensile strength also increased at a lower rate.

4.3. Flexural Strength

Figure 4.3 shows the net flexural strengths of notched beams subjected to three-point bending tests. The results varied between 6.02 MPa and 6.49 MPa. Nevertheless, the effectiveness of utilizing MK or SF can be observed. The higher the amount of MK and SF the higher the flexural strength was observed. The tendency of the influence of MK and SF appeared to be almost similar to the results of compressive strength and splitting tensile strength. Moreover, the results obtained for this test has revealed that evaluating the mechanical properties by only flexural test may be misleading due to the narrow range of the variation of the results.

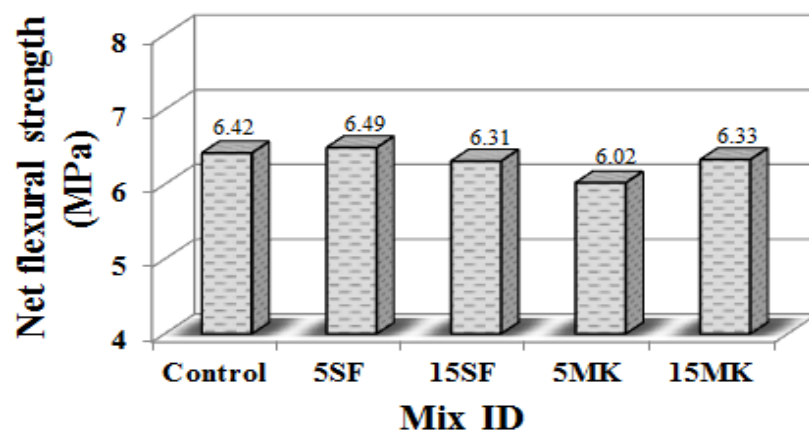


Figure 4.3 Variation in net flexural tensile strength of concretes containing SF and MK at 28 days

4.4. Modulus of elasticity

The elastic properties of concrete are surely affected by elastic properties of the ingredients and the characteristics of the interfacial zone between hardened cement paste and aggregates (Alexander and Milne, 1995). As a result of inherent stiffness and larger volume occupation in concrete, the aggregate type and strength exerts a significant influence on the elastic modulus of concrete. However, not only aggregate properties, but also the quality of the paste is another important factor characterizing the elastic behavior. Therefore, it can be inferred that, the higher the quality of cement paste and interfacial transition zone, the higher the elastic properties can be observed. The test results regarding the effect of MK and SF on modulus of elasticity of concrete were given in Figure 4.4. The lowest modulus of elasticity was observed for control concrete as 41.7 GPa, while mineral admixed concretes revealed 11% to 28% increase mainly depending on type and replacement level of the mineral admixture used.

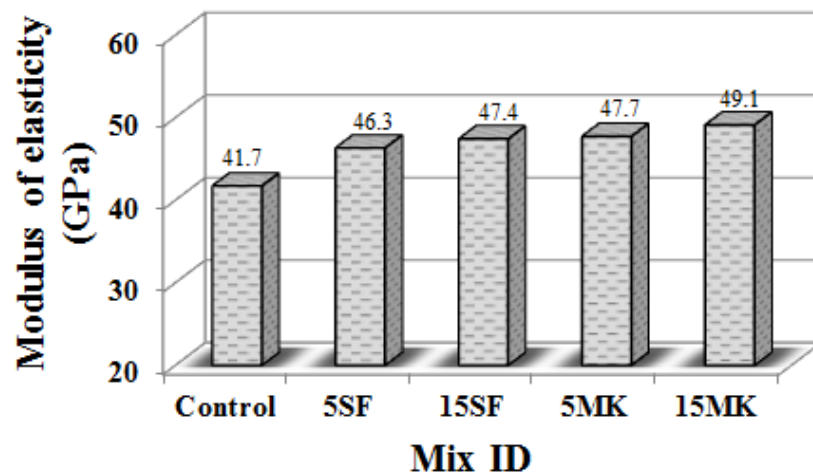


Figure 4.4 Variation in modulus of elasticity of concretes containing SF and MK at 28 days

Unlike the test results presented above, MK modified concretes, at this time, demonstrated slightly higher elasticity modulus than SF including ones. However, it should be noted that, the results yet, very close to each other. For example, 5MK concrete had only 1.4 GPa higher modulus of elasticity than 5SF concrete. Increasing the replacement level for MK and SF resulted in only small increases; such that 2.9% and 2.3% increases were observed between 5% and 15% replacement levels for the concretes including MK and SF, respectively. Qian and Li (2001) studied the relationships between stress and strain for high-performance concrete incorporating 0%, 5%, 10%, and 15% with metakaolin. They reported that the elasticity modulus of the concretes exhibited only small increases with increase in metakaolin content.

4.2. Fracture Parameters

4.2.1. Fracture energy (G_F)

Fracture energy (G_F) can be defined as the energy required for developing one crack completely. The load–deflection curves were utilized for computing G_F . The area under the load versus deflection at mid span curve is a measure of the fracture energy of any material. G_F results calculated for concrete, in this study, are based on the area under the full load–deflection curve. The cut-off deflection value was selected as 1.5 mm. The load-deflection curves, the areas under these curves, the maximum midspan deflections, and fracture energies of the concretes are depicted in Figures 4.5-4.8. Considering the ranking from the highest to the lowest peak values, the concretes were sequenced as 15SF, 15MK, 5SF, 5MK, and control. Before reaching the peak load, the slopes of the concretes can clearly be distinguished, while post-peak behavior was somehow more sophisticated. Guinea et al.(2002) claims that it can be assumed that the initial steeper portion of the softening curve is controlled by the

cracking in the matrix. Nevertheless, no direct and quantitative evidence has been available to support these statements (Guinea et al., 2002).

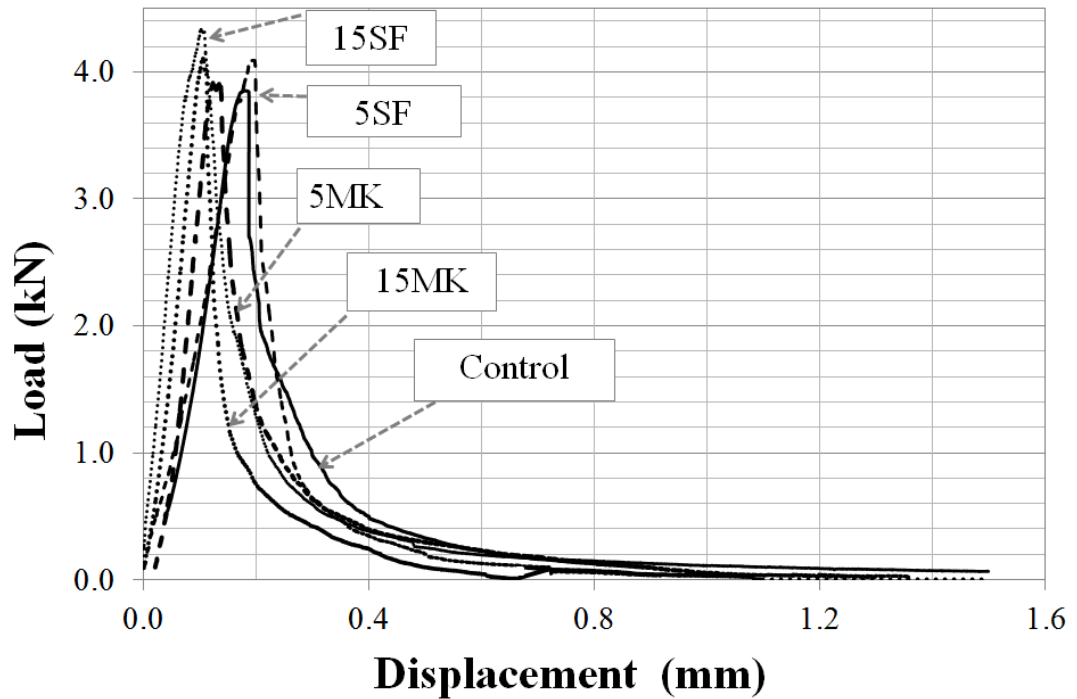


Figure 4.5 Effect of MK or SF incorporation on the load-deflection behavior of the concretes

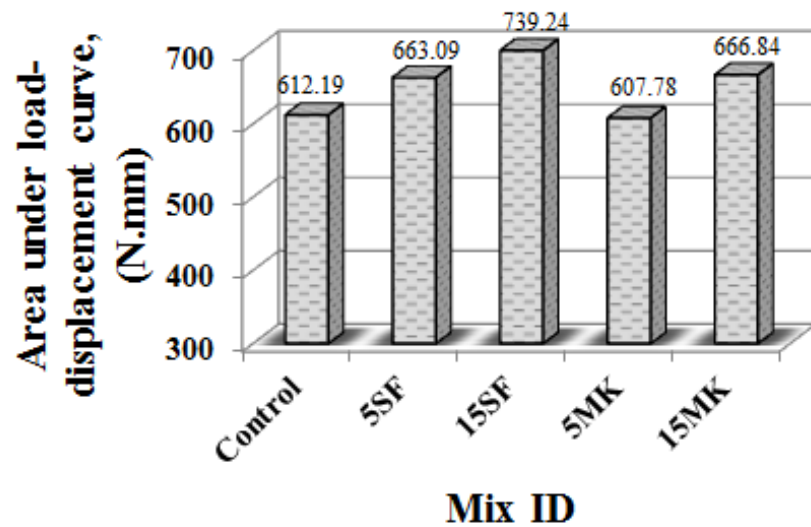


Figure 4.6 Variation in area under load-displacement curves of concretes containing SF and MK at 28 days

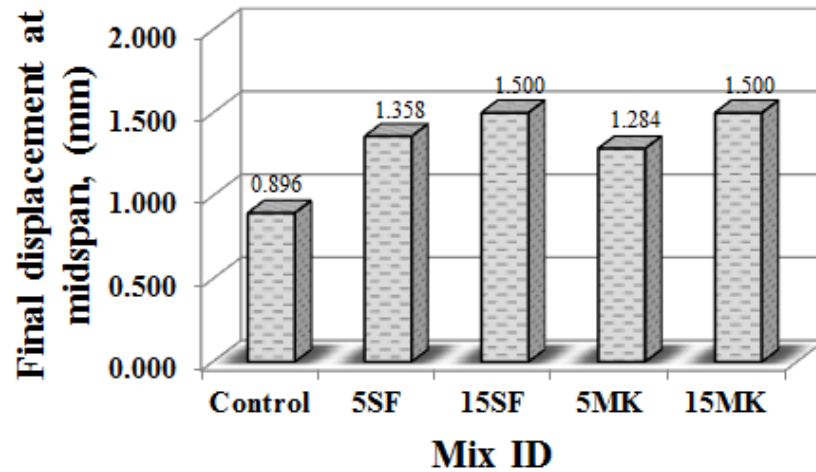


Figure 4.7 Variation in final displacement of beam specimens

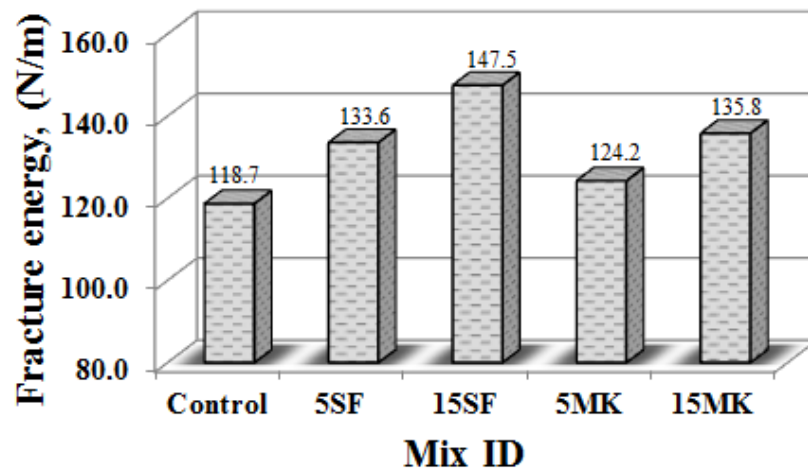


Figure 4.8 Variation in fracture energies (G_F) of the concretes containing SF and MK at 28 days

To clarify the load-deflection behavior, other parameters such as area under the curve and the maximum mid span deflection can be observed. Figure 4.6 shows that the highest area was calculated for 15SF concrete as 739 N.mm. However, the area measured for 5 MK concrete was almost same as that of control concrete. But, when observing the final displacement of the mid points (Figure 4.7), it was found out that

5MK concrete revealed 43% higher deflection than control concrete. Besides, the concretes including 15% MK or SF did not failed when the specified maximum deflection was reached. The most important contribution of MK and SF inclusion in the concrete is provision of an increase in the energy required for fracture by the resultant refinement interfacial transition zone between aggregate and cement paste.

4.2.2. Characteristic Length (l_{ch})

Being one of the most important parameter revealing ductile behavior of materials characteristic length (l_{ch}) ought to be taken into account during the design of concrete mixtures, as it provides a control on the failure mode, nominal strength, and crack formation (Lange-Kornbak and Karihaloo, 1998). The characteristics length values calculated on the basis of Eqn 3.5 are also shown in Figure 4.9. The maximum l_{ch} value of 303 mm was calculated for control concrete. In general, both SF and MK concretes yielded lower l_{ch} value, irrespective of replacement level. The divergence of l_{ch} values of the control and mineral admixed concretes were in the range of 12% to 20%. Furthermore, Although aforementioned test results indicated slightly different behavior in mechanical and fracture properties of MK and SF modified concretes, being an important parameter indicating the interaction of modulus of elasticity, fracture energy, and splitting tensile strength, the characteristic length values were almost same for the same replacement level of MK and SF.

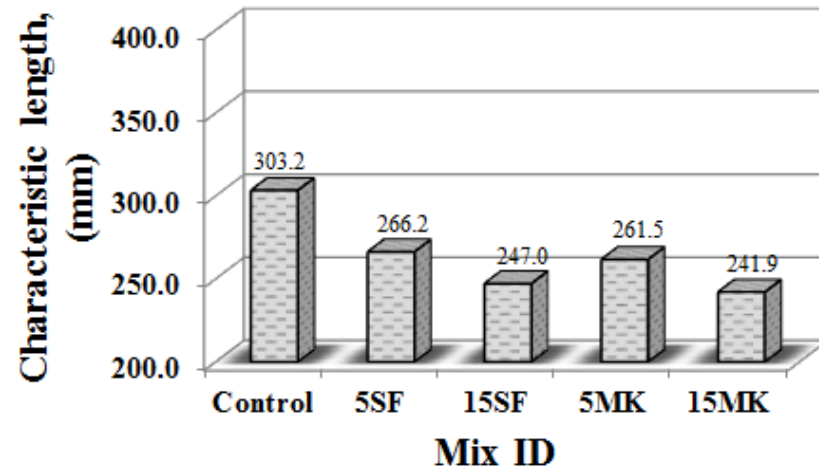


Figure 4.9 Variation in characteristic lengths of the concretes containing SF and MK at 28 days

CHAPTER 5

5. CONCLUSIONS

Based on the findings presented above the following conclusions can be drawn:

- SF and MK concretes had systematically higher compressive strength than the control concrete at 28 days. There was a consistent increase in compressive strength with the increase in MK and SF. The maximum compressive strength value of 86.8 MPa which was far higher than that of control was observed for 15SF concrete. However, based on the indirect measurement of tensile strength by splitting, it was observed that even though there is a similar tendency in tensile strength variation of the concretes to compressive strength, the differences between control and MK or SF incorporated concretes were not as high as compressive strength.
- Net flexural strength results indicated that the concretes incorporating SF reached to higher values for the same replacement levels of MK. However, both types of concrete had relatively higher flexural strength values than that of control.
- Regardless the replacement level, modulus of elasticity values of SF and MK modified concretes were close to each other. However, the modulus of elasticity measured for control concrete was up to 28% less than mineral admixed concretes at varying magnitudes.
- Load-deflection behaviors of the concretes have revealed that 15% incorporation of MK or SF provided more ductile behavior. Specimens

belonging to 15SF and 15MK concretes did not failed even at the maximum specified midspan deflection (1.5 mm). Hence, fracture energies calculated for these concretes were relatively higher than the ones incorporating 5% or no mineral admixtures.

- Being one of the most critical ductility/brittleness behaviors, the characteristic length values were observed to be almost same for the mineral admixed concretes having same replacement levels. For the control concrete, on the other hand, the maximum characteristic length was calculated. This parameter is crucial since it combines the critical mechanical parameters, such as modulus of elasticity, fracture energy, and splitting tensile strength. Therefore, it can be inferred that effectiveness MK and SF on the fracture behavior of concretes mostly similar to each other.

REFERENCES

Alexander, M.G., Milne, T.I. (1995). Influence of cement blend and aggregate type on stress– strain behavior and elastic modulus of concrete, *ACI Material Journal*, **92**, 227–234.

Alexander, M.G., Magee, B.J. (1999). Durability performance of concrete containing condensed silica fume, *Cement and Concrete Research*, **29**, 917-22.

Al-Khaja, W.A. (1994). Strength and time-dependent deformations of silica fume concrete for use in Bahrain, *Construction and Building Materials*, **8**, 169-172.

Almusallam, A.A, Beshr, H., Maslehuddin, M., Al-Amoudi, O. S.B. (2004). Effect of silica fume on the mechanical properties of low quality coarse aggregate concrete, *Cement & Concrete Composites*, **26**, 891–900.

ASTM C192/C192M-07. American Society for Testing and Materials. 2007 Standard Practice for Making and Curing Concrete Test Specimens in the Laboratory. Annual Book of ASTM Standard, Philadelphia, Vol. 04-02, 8 pages.

ASTM C39/C39M-12. American Society for Testing and Materials. 2012 Standard Test Method for Compressive Strength of Cylindrical Concrete Specimens. Annual Book of ASTM Standard, Philadelphia, Vol. 04-02, 7 pages.

ASTM C496. American Society for Testing and Materials. 2011 Standard Test Method for Splitting Tensile Strength of Cylindrical Concrete Specimens. Annual Book of ASTM Standard. Philadelphia, Vol. 04-02, 5 pages.

ASTM C469/C469M-10. American Society for Testing and Materials. 2010. Standard Test Method for Static Modulus of Elasticity and Poisson's Ratio of Concrete in Compression. Book of Standards Volume:04.02, 5 pages.

Barenblatt, G.I. (1962). The mathematical theory of equilibrium cracks in brittle fracture, *Advances in Applied Mechanics*, **7**, 55-129.

Badogiannis, E., Kakali, G., Tsivilis, S. (2005). Metakaolin as a supplementary cementitious material; optimization of kaolin to metakaolin conversion, *J of Ther Anal and Cal*, **81**, 457-62.

Barnes, P., Bensted, J., Jones, T.R. (2003). Structure and performance of cements. 2nd edition. Metakaolin as pozzolanic addition to concrete. England. p. 372-98.

Bazant, Z.P., Oh, B.H. (1983). Crack band theory for fracture of concrete, *Materials and Structure*, **93**, 155-177.

Bazant, Z.P. (1984). Size effect in blunt fracture: Concrete, rock, metal, *Journal Engineering Mechanics ASCE*, **4**, 518-535.

Bazant, Z.P., Kim, J.K., Pfeiffer, P.A. (1986). Determination of fracture properties from size effect tests, *Journal Structure Engineering ASCE*, **2**, 289-307.

Bazant, Z.P., Cedolin, L., (1991). *Stability of Structures*, Oxford University Press, New York, p. 917.

Bhanjaa, S, Sengupta, B . (2005). Influence of silica fume on the tensile strength of concrete, *Cement and Concrete Research*, **35**, 743–747.

Bazant, Z.P., (2004). Proceedings of the Academy of Sciences, **101**, 13400–13407.

Bache, H.H., (1986). Fracture Mechanics in Design of Concrete Structures, in *Fracture Toughness and Energy of Concrete*, Wittman, F.H., ed., Elsevier, Amsterdam, p. 582.

Caldarone, M.A., Gruber, K.A., Burg, R.G. (1994). High-reactivity metakaolin: a new generation mineral admixture, *Concrete Internationa.*, **16**, 37–40.

Cedolin, L., (1986). Introduction to Fracture Mechanics of Concrete, *El Cemento*. **4**,285, 1986.

Dugdale, D.S. (1960). Yielding of steel sheets containing slits, *Journal Mechanics Phys Solid*, **8**,100-104.

Ding, J.T. and Li, Z. (2002). Effects of metakaolin and silica fume on properties of Concrete, *ACI Materials Journal*, **90**, 393-398.

Güneyisi, E., Mermerdaş, K. (2007). Comparative study on strength, sorptivity, and chloride ingress characteristics of air-cured and water-cured concretes modified with metakaolin, *Materials and Structure*, **40**, 1161-1171.

Güneyisi, E., Gesoğlu, M., Mermerdaş, K. (2008). Improving strength, drying shrinkage, and pore structure of concrete using metakaolin, *Materials and Structure*, **41**, 937-49.

Güneyisi, E., Gesoğlu, M., Mermerdaş, K. (2010). Strength deterioration of plain and metakaolin concretes in aggressive sulfate environments, *ASCE Journal of Materials in Civil Engineering*, **22**, 403-407.

Güneyisi, E., Gesoğlu, M., Karaoğlu, S., Mermerdaş, K. (2012) Strength, permeability and shrinkage cracking of silica fume and metakaolin concretes, *Construction and Building Materials*, **34**, 120-130.

Güneyisi, E., Gesoğlu, M., Özturan, T., Mermerdaş, K. (2012). Microstructural properties and pozzolanic activity of calcined kaolins as supplementary cementing materials. *Canadian Journal Civil Engineering*, **39**, 1274-1284.

Güneyisi, E., Gesoğlu, M., Karaboğa, F., Mermerdaş, K. (2013). Corrosion behavior of reinforcing steel embedded in chloride contaminated concretes with and without metakaolin. *Composites: Part B*, **45**, 1288–1295.

Guinea, G.V., El-Sayed, K., Rocco, C.G., Elices, M., Planas J. (2002). The effect of the bond between the matrix and the aggregates on the cracking mechanism and fracture parameters of concrete, *Cement and Concrete Research*, **32**,1961–1970.

Ghorpade, V.G. and Rao, H.S. (2011). Chloride ion permeability studies of metakaolin based high performance concrete, *International Journal of Engineering Science and Technology*, **3**, 0975-5462.

Hariharan, A.R., Santhi, A.S., Ganesh, G.M.(2011). Study on Strength Development of High Strength Concrete Containing Fly ash and Silica fume, *International Journal of Engineering Science and Technology*, **3**, 0975-5462.

Hubertova, M., Hela, R. (2007). The effect of metakaolin and silica fume on the properties of lightweight self-consolidating concrete. ACI Publication SP-243- 3, Detroit: American Concrete Institute. p. 35-48.

Hillerborg, A., Modeer, M., Petersson, P.E. (1976). Analysis of crack formation and crack growth in concrete by means of fracture mechanics and finite elements, *Cement and Concrete Research*, **6**, 773–782.

Indian Standard IS 5816 (1999). Splitting tensile strength of concrete method of test.

Irwin, G.R. (1957). Analysis of stresses and strain near the end of crack transverse a plate, *Journal of applied Mechanics*, **24**, 361-364.

Justice, J.M., Kennison, L.H., Mohr, B.J., Beckwith, S.L., McCormick, L.E., Wiggins, B., Zhang, Z.Z., and Kurtis, K.E. (2005). Comparison of Two Metakaolins and a Silica Fume Used as Supplementary Cementitious Materials, *Proc. Seventh International Symposium on Utilization of High-Strength/High Performance Concrete*, to be held in Washington D.C.

Jenq, Y.S., Shah, S.P. (1985). Two parameter fracture model for concrete, *Journal of Engineering Mechanics ASCE*, **10**, 1227-1241.

Kaplan, M.E. (1961). Crack propagation and fracture of concrete, *Journal of American concrete Institute*, **58**, 591-610.

Kakali, G., Perraki, T., Tsivilis, S., Badogiannis, E. (2001). Thermal treatment of kaolin: the effect of mineralogy on the pozzolanic activity, *Appl Clay Sci*, **20**, 73-80.

Kostuch, J.A., Walters, G.V., Jones, T.R. (1993). High performance concrete incorporating metakaolin: a Review. In: Dhir RK, Jones MR, editors. *Concrete. E & FN Spon*, p. 1799–811.

Khatri, R.P., Sirivivatnanon, V., Yu, L.K. (1997). Effect of curing on water permeability of concretes prepared with normal portland cement and with slag and silica fume, *Magazine of Concrete Research*, **49**, 167-172.

Kim, H.S., Lee, S.H., Moon, H.Y. (2007). Strength properties and durability aspects of high strength concrete using Korean metakaolin, *Construction and Building Materials*, **21**, 1229–1237.

Kumar, S. and Barai, S.V. (2011). Concrete fracture models and application. Berlin. Springer.

Lange-Kornbak, D., Karihaloo, B.L. (1998). Design of fibre-reinforced DSP mixes for minimum brittleness, *Adv Cem Based Mater*, **7**, 89– 101.

Lee, S.T., Moon, H.Y., Hooton, R.D., Kim, J.P. (2005). Effect of solution concentrations and replacement levels of metakaolin on the resistance of mortars exposed to magnesium sulfate solutions, *Cement and Concrete Research*, **35**, 1314-1323.

Mermerdaş, K., Gesoğlu, M., Güneyisi, E., Özturan, T. (2012). Strength development of concretes incorporated with metakaolin and different types of calcined kaolins, *Construction and Building Materials*, **37**, 766–774.

Mehta, P.K., Monteiro, P.J.M.(2006). Concrete: Microstructure, Properties, and Materials. 3rd Edition, USA, McGraw-Hill.

Murali, G. and Sruthee, P. (2012). Experimental study of concrete with metakaolin as partial replacement of cement of concrete, *International Journal of Emerging Trends in Engineering and Development*, **2**, 2249-6149.

Nallathambi, P., Karihaloo, B.E. (1986). Determination of specimen-size independent fracture toughness of plain concrete. *Magazine Concrete Research*, **38**, 67-76.

Neville, A.M. (1996). *Properties of Concrete*. 4th and final ed., Addison Wesley Logman, England.

Noguchi. T., Nemati. K. M. (1990). Relationship between compressive strength and modulus of elasticity of high strength concrete.

http://enpub.fulton.asu.edu/cement/cbm_CI/CBMI_Separate_Articles/Article-50.pdf

Peterson, P.E. (1980). Fracture energy of concrete: method of determination, *Cement and Concrete Research*, **10**, 79-89.

Poon, C.S., Kou, S.C., Lam, L. (2006). Compressive strength, chloride diffusivity and pore structure of high performance metakaolin and silica fume concrete, *Construction and Build Materials*, **20**, 858–65.

Rao, G.A., Prasad, B.K.R.(2002). Fracture energy and softening behavior of high-strength concrete, *Cement and Concrete Research*, **32**, 247–252.

Ramachandran, V.S. (1996). *Concrete admixtures handbook: properties, science, and technology*. 2nd Edition. USA. Noyes Publications.

RILEM 50-FMC. (1985). Committee of fracture mechanics of concrete. Determination of fracture energy of mortar and concrete by means of three-point bend tests on notched beams, *Material and Structure*, **18**, 285–90.

Sabir, B.B., Wild, S., Bai, J. (2001). Metakaolin and calcined clays as pozzolans for concrete: a review, *Cement Concrete Composite*, **23**, 441-454.

Shekarchi, M., Bonakdar, A., Bakhshi, M., Mirdamadi, A., Mobasher, B. (2010). Transport properties in metakaolin blended concrete, *Construction Building Materials*, **24**, 2217–2223.

Shvarzman, A., Kovler, K., Grader, G.S., Shter, G.E. (2003). The effect of dehydroxylation/amorphization degree on pozzolanic activity of kaolinite, *Cement Concrete Research*, **31**, 405-416.

Saeed Karim Babanajad, Yaghoob Farnam, Mohammad Shekarchi. (2012). Failure criteria and triaxial behaviour of HPFRC containing high reactivity metakaolin and silica fume, *Construction and Building Materials*. **29**, 215–229.

Si-Ahmed, M., Belakrouf, A., and Kenai, S. (2012). Influence of Metakaolin on the Performance of Mortars and Concretes. World Academy of Science, *Engineering and Technology*, **71**, 1354-1357.

Shah, S.R., Swartz, S.E., Ouyang, C. (1995). *Fracture Mechanics of Concrete: Applications of Fracture Mechanics to Concrete, Rock and Other Quasi-Brittle Materials*. Wiley, New York, NY.

Şahin, Y., Köksal, F. (2011). The influence of matrix and steel fiber tensile strength on the fracture energy of high-strength concrete, *Construction and Building Materials*, **25**, 1801-1806.

VU, D.D. (2002). Strength properties of metakaolin blended paste, mortar and concrete. PhD Thesis. Hanoi Polytechnic University.

Wild, S., Khatip, J.M., Jones, A. (1996). Relative strength, pozzolanic activity and cement hydration in superplasticized metakaolin concrete, *Cement and Concrete Research*. **26**, 1537-1544.

Wu, K., Chen, B., Yao, W., Zang, D. (2001). Effect of coarse aggregate type on mechanical properties of high-performance concrete, *Cement and Concrete Research*, **31**, 1421-1425.

Qian, X., and Li, Z., (2001). The relationships between stress and strain for high-performance concrete with metakaolin, *Cement and Concrete Research*, **31**, 1607–1611.

Xu, S., Reinhardt, I.I.W. (1998). Crack extension resistance and fracture properties of quasi-brittle materials like concrete based on the complete process of fracture, *International Journal of Fracture*, **92**, 71-99.

Xu, S., Reinhardt, I.I.W. (1999). Determination of double- K criterion for crack propagation in quasi-brittle materials, part I: Experimental investigation of crack propagation, *International Journal of Fracture*, **98**, 111-149.

Xu, S., Zhang, X. (2008). Determination of fracture parameters for crack propagation in concrete using an energy approach, *Engineering Fracture Mechanics*, **75**, 4292—1308.

Yajun, Ji., Cahyadi, J.H. (2003). Effects of densified silica fume on microstructure and compressive strength of blended cement pastes, *Cement and Concrete Research*, **33**, 1543–1548.

Zhang, M.H., Malhotra, V.M. (1995). Characteristics of a thermally activated alumino-silicate pozzolanic material and its use in concrete, *Cement and Concrete Research*, **25**, 1713-1725.